A_1 adenosine receptor-induced phosphorylation and modulation of transglutaminase 2 activity in H9c2 cells: a role in cell survival

Falguni S. VYAS, Alan J. HARGREAVES, Philip L. R. BONNER, David J. BOOCOCK[1], Clare COVENEY[1], John M. DICKENSON*

School of Science and Technology
Nottingham Trent University
Clifton Lane
Nottingham
NG11 8NS

[1]John van Geest Cancer Research Centre
Nottingham Trent University
Clifton Lane
Nottingham
NG11 8NS

*To whom correspondence should be addressed

Tel: +44-1158486683

E-mail: john.dickenson@ntu.ac.uk

Classification**:** Cardiovascular Pharmacology

Abstract

The regulation of tissue transglutaminase (TG2) activity by the GPCR family is poorly understood. In this study, we investigated the modulation of TG2 activity by the A_1 adenosine receptor in cardiomyocyte-like H9c2 cells.H9c2 cells were lysed following stimulation with the A_1 adenosine receptor agonist N^6-cyclopentyladenosine (CPA). Transglutaminase activity was determined using an amine incorporating and a protein cross linking assay. TG2 phosphorylation was assessed via immunoprecipitation and Western blotting. The role of TG2 in A_1 adenosine receptor-induced cytoprotection was investigated by monitoring hypoxia-induced cell death. CPA induced time and concentration-dependent increases in amine incorporating and protein crosslinking activity of TG2. CPA-induced increases in TG2 activity were attenuated by the TG2 inhibitors Z-DON and R283. Responses to CPA were blocked by PKC (Ro 31-8220), MEK1/2 (PD 98059), p38 MAPK (SB 203580) and JNK1/2 (SP 600125) inhibitors and by removal of extracellular Ca^{2+}. CPA triggered robust increases in the levels of TG2-associated phosphoserine and phosphothreonine, which were attenuated by PKC, MEK1/2 and JNK1/2 inhibitors. Fluorescence microscopy revealed TG2-mediated biotin-X-cadaverine incorporation into proteins and proteomic analysis identified known (Histone H4) and novel (Hexokinase 1) protein substrates for TG2. CPA pre-treatment reversed hypoxia-induced LDH release and decreases in MTT reduction. TG2 inhibitors R283 and Z-DON attenuated A_1 adenosine receptor-induced cytoprotection. TG2 activity was stimulated by the A_1 adenosine receptor in H9c2 cells via a multi protein kinase dependent pathway. These results suggest a role for TG2 in A_1 adenosine receptor-induced cytoprotection.

Key words:

A_1 adenosine receptor, cytoprotection, G protein-coupled receptor, transglutaminase 2, SWATH mass spectrometry.

Abbreviations:

BSA, bovine serum albumin; CPA, N^6-cyclopentyladenosine; DAG, diacylglycerol; DMEM, Dulbecco's modified Eagle's medium; DPCPX, 8-cyclopentyl-1,3-dipropylxanthine, EDTA, ethylenediaminetetraacetic acid; ERK1/2, extracellular signal-regulated kinases 1 and 2; FITC, fluorescein isothiocyanate; GPCRs, G-protein coupled receptors; HRP, horseradish peroxidase; IGEPAL CA-630, octylphenyl-polyethylene glycol; JNK, c-Jun N-terminal kinase; LDH, lactate dehydrogenase; MAPK, mitogen activated protein kinase; MEK1/2, mitogen-activated protein kinase kinase 1/2; MKK4/7, mitogen activated protein kinase kinase 4 and 7; MTT, 3-(4-5-dimethylthiazol2-yl)-2,5-diphenyltetrazolium bromide; PBS, phosphate-buffered saline; PD 98059, 2′-amino-3'-methoxyflavone; PI-3K, phosphatidylinositol 3-kinase; PKB, protein kinase B; PKA, protein kinase A; PKC, protein kinase C; PMA, phorbol-12-myristate-13-acetate; R283, 1,3-dimethyl-2[(2-oxopropyl)thio]imidazolium chloride; Ro 31-8220, 3-{1-[3-(2-isothioureido) propyl]indol-3-yl}-4-(1-methylindol-3-yl)-3-pyrrolin-2,5-dione; SB 203580, 4-(4-fluorophenyl)-2-(4-methylsulfinylphenyl)-5-(4-pyridyl)1H-imidazole; SDS-PAGE, sodium dodecyl sulphate polyacrylamide gel electrophoresis; SP 600125, anthra[1-9-*cd*]pyrazol-6(2*H*)-one; SWATH-MS, Sequential Windowed Acquisition of All Theoretical Fragment Ion Mass Spectra; TG2, transglutaminase type 2; Z-DON, benzyloxycarbonyl-(6-Diazo-5-oxonleucinyl)-L-valiyl-L-prolinyl-L-leucinmethylester.

1. Introduction

Transglutaminases (TGs) comprise a family of calcium (Ca^{2+}) dependent enzymes (TG1-7 and Factor XIIIa) that catalyse post-translational modification of proteins. Once Ca^{2+} binds to TG, a cysteine is exposed leading to the formation of a bond between ε-amide (as an isodipeptide or polyamine bond) and γ-carboxamide of protein bound glutamine residues [1]. Transglutaminase 2 (TG2), the most widely studied member of the TG family, has been implicated in the regulation of a wide range of processes, including cell adhesion, migration, growth, survival, apoptosis, differentiation, and extracellular matrix organization [2]. The role of TG2 in cell survival and cell death is cell-specific with respect to whether it has pro- or anti-apoptotic effects [3]. Dysregulation of TG2 occurs in many pathologies, including coeliac disease, neurodegenerative disorders, some cancers and, as such, represents a potential therapeutic target [4].

Transglutaminase 2 possesses multiple enzymic functions that include transmidation, protein disulphide isomerase and protein kinase activity [5]. The transamidase activity of TG2 is inhibited by GTP/GDP and when bound to GTP/GDP, TG2 functions as a G-protein known as Gh independently of its transamidase activity [6]. Interestingly, the activity of TG2 and other TGs can be regulated by protein kinases. For example, phosphorylation of TG2 by protein kinase A (PKA) inhibits its transamidating activity but enhances its kinase activity [7], whereas cross-linking activity of TG1 is enhanced by phorbol ester-induced stimulation of protein kinase C (PKC) and extracellular signal-regulated kinases 1 and 2 (ERK1/2) [8]. Finally, PKC-δ has been shown to regulate TG2 expression in pancreatic cancer cells [9]. Overall, these observations suggest that the activity and expression of specific TG isoenzymes can be regulated by signaling pathways associated with G-protein coupled receptors (GPCRs). However, little is currently known about the regulation of TG2 enzymic activity following GPCR stimulation.

The A_1 adenosine receptor is a member of the GPCR superfamily, which couples to pertussis toxin-sensitive G_i/G_o-proteins [10]. Although the A_1 adenosine receptor stimulation is traditionally associated with inhibition of adenylyl cyclase, it also triggers the activation of additional signalling cascades involving PKC, PKB, ERK1/2, and p38 MAPK [11-16]. Since PKC and ERK1/2 pathways are associated with modulation of TG activity [7,8], it is conceivable that the A_1 adenosine receptor regulates TG activity. Since H9c2 cells express functional A_1 adenosine receptors [17] the primary aims of this study were (i) to determine whether the A_1 adenosine receptor modulates TG2 activity in these cells, and (ii) whether TG2 is involved in A_1 adenosine receptor induced cytoprotection [17]. The results obtained indicate that A_1 adenosine receptor stimulation

modulates TG2 phosphorylation and activity via a multi protein kinase and extracellular Ca^{2+}-dependent pathway.

2. Materials and methods

2.1. Materials

BAPTA/AM, forskolin, PD 98059, Ro-31-8220 ({3-[1-[3-(amidinothio) propyl-1H-indol-3-yl]-3-(1-methyl-1H-indol-3-yl)maleimide bisindolylmaleimide IX, methanesulfonate}) SB 203580, SP 600 125, and thapsigargin were obtained from Tocris Bioscience (Bristol, UK). Adenosine, casein, DPCPX (1,3-dipropylcyclopentylxanthine), IGEPAL, MTT (3-(4-5-dimethylthiazol-2-yl)-2,5-diphenyltetrazolium bromide), N^6-cyclopentyladenosine, N',N'-dimethylcasein, paraformaldehyde, pertussis toxin, protease inhibitor cocktail, phosphatase inhibitor cocktail 2 and 3, ExtrAvidin®-HRP and ExtrAvidin®-FITC and Triton™ X-100 were obtained from Sigma-Aldrich Co. Ltd. (Gillingham, UK). Fluo-8/AM was purchased from Stratech Scientific Ltd (Newmarket, UK). The TG2 inhibitors Z-DON (Z-ZON-Val-Pro-Leu-OMe) and R283 along with purified standard guinea-pig liver TG2 were obtained from Zedira GmbH (Darmstadt, Germany). Biotin-TVQQEL was purchased from Pepceuticals (Enderby, UK). DAPI was from Vector Laboratories Inc (Peterborough, UK). Coomassie blue (InstantBlue™ stain) was purchased from Expedeon (Swavesey, UK). Biotin cadaverine (N-(5-Aminopentyl)biotinamide) and biotin-X-cadaverine(5-([(N-(Biotinoyl)amino)hexanoyl]amino)pentylamine) were purchased from Invitrogen UK (Loughborough, UK). DMEM (Dulbecco´s modified Eagle´s medium), foetal bovine serum, trypsin (10X), L-glutamine (200 mM), penicillin (10,000 U/ml)/streptomycin (10,000 μg/ml) were purchased from Lonza, (Castleford, UK). All other reagents were purchased from Sigma-Aldrich Co. Ltd. (Gillingham, UK) and were of analytical grade. Antibodies were obtained from the following suppliers: monoclonal phospho-specific ERK1/2 (Thr^{202}/Tyr^{204}) from Sigma-Aldrich Co. Ltd; polyclonal phospho-specific PKB (Ser^{473}), polyclonal total unphosphorylated PKB, monoclonal total unphosphorylated ERK1/2, polyclonal total unphosphorylated JNK, polyclonal total unphosphorylated p38 MAPK, monoclonal phospho-specific p38 MAPK and monoclonal phospho-specific JNK were from New England Biolabs (UK) Ltd (Hitchin, UK); monoclonal anti-TG2 (CUB 7402) from Thermo Scientific (Leicestershire, UK); polyclonal anti-phosphoserine and polyclonal anti-phosphothreonine from Abcam (Cambridge, UK).

2.2. Cell Culture

Rat embryonic cardiomyoblast-derived H9c2 cells were obtained from the European Collection of Animal Cell Cultures (Porton Down, Salisbury, UK). These cells, derived from embryonic rat heart tissue [18], are increasingly used as an *in vitro* model for studies exploring cardioprotection since they display similar morphological, electrophysiological and biochemical properties to primary cardiac myocytes [19]. Cells were cultured in DMEM supplemented with 2 mM L-glutamine, 10% (v/v) foetal bovine serum and penicillin (100 U/ml)/streptomycin (100 μg/ml). They were maintained in a humidified incubator (95%

air/5% CO_2 at 37°C) until 70-80% confluent and sub-cultured (1:5 split ratio) using trypsin (0.05% w/v)/EDTA (0.02% w/v). Experiments were performed on passage numbers 2-28.

2.3. Transglutaminase activity assays

Time course profiles and concentration-response response curves were obtained for CPA and adenosine. Where appropriate, cells were also pre-incubated for 30 min in medium with or without the protein kinase inhibitors Ro 31-8220 (PKC; 10 μM; [20]), PD 98059 (MEK1/2, 50 μM; [21]), SB 203580 (p38 MAPK; 20 μM; [22]), and SP 600 125 (JNK1/2; 20 μM; [23]) prior to treatment with 100 nM CPA or 100 μM adenosine. Following stimulation, cells were rinsed twice with 2.0 ml of chilled PBS, lysed with 500 μl of ice-cold lysis buffer (50 mM Tris-HCl pH 8.0, 0.5% (w/v) sodium deoxycholate, 0.1% (v/v) protease inhibitor cocktail, and 1% (v/v) phosphatase inhibitor cocktail 2). Cell lysates were clarified by centrifugation at 4°C for 10 min at 14000 x g prior to being assayed for TG2 activity, as described below. Protein was determined using the bicinchoninic acid (BCA) protein assay [24], using a commercially available kit (Sigma-Aldrich Co. Ltd), with bovine serum albumin (BSA) as the standard

Biotin-labeled cadaverine-incorporation assays were performed according to Slaughter *et al.* [25] with modifications [26], as described previously [27]. The biotin-labeled peptide cross-linking assay was performed according to the method of Trigwell *et al.* [28] with minor modifications [27]. The reaction was started by the addition of 50 μl of samples, positive control (50 ng/well of guinea-pig liver TG2) or negative control (100 mM Tris-HCl, pH 8.0) and allowed to proceed for 1 h at 37°C. In both assays, the reaction was terminated by adding 50 μl of 5.0 M sulphuric acid and the absorbance read at 450 nm. One unit of TG2 was defined as a change in absorbance of one unit h^{-1}.

2.4. Hypoxia-induced cell death

H9c2 cells in glucose-free and serum-free DMEM (Gibco™, Life Technologies Ltd, Paisley, UK) were exposed to 8 h hypoxia using a hypoxic incubator (5% CO_2/1% O_2 at 37°C) in which O_2 was replaced by N_2.

2.5. Cell viability assays

H9c2 cells were plated in 24-well flat bottomed plates (15,000 cells per well) and cultured for 24 h in fully supplemented DMEM, before cell viability was determined by measuring the reduction of MTT [29]. The amount of DMSO-solubilised reduced formazan product was determined by measurement of absorbance at a wavelength 570 nm. Alternatively, cells were plated in 96-well flat bottomed plates (5,000 cells per well) and incubated as above.

Following normoxia/hypoxia exposure, the activity of lactate dehydrogenase (LDH) released into the culture medium was detected using the CytoTox 96®non-radioactive cytotoxicity assay (Promega, Southampton, UK) with measurement of absorbance at 490 nm.

2.6. SDS-polyacrylamide gel electrophoresis and Western blot analysis

Protein samples (15-20 µg) were separated by SDS-PAGE in 10% (w/v) polyacrylamide gels using a Bio-Rad Mini-Protean III system. Proteins were transferred to nitrocellulose membranes in a Bio-Rad Trans-Blot system, using electro-transfer buffer comprising 25 mM Tris, 192 mM glycine pH 8.3 and 20% (v/v) MeOH. Following transfer, the membranes were blocked and probed with antibodies as described by Alamami et al. [27]. The primary antibodies (1:500 dilutions unless otherwise indicated) used were phospho-specific ERK1/2 (1:1000), phospho-specific PKB, phospho-specific p38 MAPK, phospho-specific JNK. Horseradish peroxidase-conjugated secondary antibodies (New England Biolabs (UK) Ltd), diluted 1:1000 in blocking buffer, were applied for 2h at room temperature. Following removal of the unbound secondary antibody, blots were extensively washed and developed using the Enhanced Chemiluminescence (ECL) Detection System (Uptima, Interchim, France) and quantified by densitometry using Advanced Image Data Analysis Software (Fuji; version 3.52). Samples were also analysed using primary antibodies that recognise total ERK1/2, PKB, p38 MAPK and JNK (1:1000) in order to confirm the uniformity of protein loading.

2.7. Measurement of *in situ* TG2 activity

H9c2 cells were seeded on 8-well chamber slides (15,000 cells well^{-1}) and cultured for 24 h in fully supplemented DMEM. The cells were then incubated for 6 h in medium containing 1 mM biotin-X-cadaverine (a cell permeable TG2 substrate; [30]) before experimentation. Where appropriate, cells were treated for 1 h with TG2 inhibitors Z-DON (150 µM) or R283 (200 µM) before the addition of 100 nM CPA or 100 µM adenosine. Following stimulation, cells were fixed with 3.7 % (w/v) paraformaldehyde and permeabilised with 0.1% (v/v) Triton-X100, both in PBS, for 15 min at room temperature. After washing, cells were blocked with 3% (w/v) BSA for 1 h at room temperature and the transglutaminase-mediated biotin-X-cadaverine labeled protein substrates detected by incubation with (1:200 v/v) FITC-conjugated ExtrAvidin® (Sigma-Aldrich Co. Ltd). Nuclei were stained with DAPI and images acquired using a Leica TCS SP5 II confocal microscope (Leica Microsystems, GmbH, Manheim, Germany) equipped with a 20x air objective. Optical sections were typically 1-2 µm and the highest fluorescence intensity was acquired using forskolin (10 µM) as a positive control [27]. Image analysis and quantification were carried out using Leica LAS AF software.

2.8. Measurement of intracellular calcium

H9c2 cells were plated in 24-well flat-bottomed plates (15,000 cells well^{-1}) and cultured for 24 h in fully supplemented DMEM. Cells were loaded with Fluo-8 AM (5 μM, 30-40 min) before mounting on the stage of an Leica TCS SP5 II confocal microscope (Leica Microsystems, GmbH, Manheim, Germany) equipped with a 20x air objective. Cells were incubated at 37°C using a temperature controller and micro incubator (The Cube, Life Imaging Services, Basel, Switzerland) in the presence of imaging buffer (134 mM NaCl 134, 6 mM KCl 6, 1.3 mM $CaCl_2$ 1 mM $MgCl_2$ 1, 10 mM HEPES, and 10 mM glucose; pH 7.4. Using an excitation wavelength of 490 nm , emissions over 514 nm were collected. Images were collected every 1.7 s for 10 min. Increases in intracellular Ca^{2+} were defined as F/F_0 where F was the fluorescence at any given time, and F_0 was the initial basal level of Ca^{2+}.

2.9. Determination of TG2 phosphorylation

Following stimulation, H9c2 cells were rinsed twice with 2.0 ml of chilled PBS and lysed with 500 μl of ice-cold lysis buffer (2mM EDTA, 1.5 mM $MgCl_2$, 10% (v/v) glycerol, 0.5% (v/v) IGEPAL, 0.1% (v/v) protease inhibitor cocktail, and 1% (v/v) phosphatase inhibitor cocktail 2 and 3 in PBS). Cell lysates were clarified by centrifugation (4°C for 10 min at 14000 x g), after which 500 μg of supernatant protein were incubated overnight at 4°C with 2 μg of anti-TG2 monoclonal antibody or IgG. Immune complexes were precipitated using Pierce™ Classic Magnetic IP/Co-IP Kit (Loughborough, UK). The precipitates were resolved by SDS-PAGE and Western blotting, then probed using anti-phosphoserine or anti-phosphothreonine antibodies (1:1000). Antibody reactivity was visualised by ECL and quantified densitometrically, as described above.

2.10. Measurement of biotin-X-cadaverine incorporation into proteins serving as substrates for TG2

Cellular proteins acting as substrates for endogenous TG2-catalysed polyamine incorporation reactions were investigated as described by Singh *et al.* [31]. Biotin-cadaverine labelled proteins were enriched using CaptAvidin™-agarose sedimentation beads (Life Technologies, UK), subjected to SDS-PAGE and separated proteins stained with Coomassie blue.

2.11. Proteomic analysis of TG2 biotin-cadaverine labelled substrate proteins

Following pre-treatment with 1 mM biotin-X-cadaverine Hc92 cells were treated with CPA or adenosine and extracted as described above. The proteins labelled with biotin-X-

cadaverine were purified using CaptAvidin™-agarose and biotin-cadaverine labelled proteins were processed for trypsin digestion (trypsin gold; Promega, Southampton, UK). Samples (~50 µg protein) were reduced and alkylated (1 µl 0.5 M DTT, 56° C for 20 min; 2.7 µl 0.55 M iodoacetamide, room temperature 15 min in the dark), dried in a vacuum concentrator (Eppendorf, UK) and resuspended in 100 µl 50 mM tri-ethyl ammonium bicarbonate (TEAB). Sigma Trypsin (2 µg) was added in 2 µl of 1 mM HCl, and incubated overnight at 37° C in a thermomixer. Samples were then evaporated to dryness in a vacuum concentrator and resuspended in 5% (v/v) acetonitrile/0.1% (v/v) formic acid (20 µl) and transferred to a HPLC vial for MS analysis. Samples (3 µl) were injected by autosampler (Eksigent nanoLC 425 LC system) at 5 µl/min onto a YMC Triart-C18 column (25 cm, 3 µm, 300 µm i.d.) using gradient elution (2-40% Mobile phase B, followed by wash at 80% B and re-equilibration) over either 110 (120 min run time) min (for spectral library construction using data/information dependent acquisition DDA/IDA) or 50 min (60 min run time) for SWATH/DIA (Data Independent Acquisition) analysis [32]. Mobile phases consisted of A: 2% (v/v) acetonitrile, 5% (v/v) DMSO in 0.1% (v/v) formic acid; B: acetonitrile containing 5% (v/v) DMSO in 0.1% (v/v) formic acid.

A spectral library was constructed using the output from ProteinPilot 5 (SCIEX) combining 4 IDA runs per group (Control, CPA treated) and filtered and aligned to spiked in iRT peptides (Biognosys, Switzerland) using PeakView 2.0 (SCIEX). SWATH data extraction, quantitation and fold change analysis were carried out using SCIEX OneOmics cloud processing software [33].

2.12. Statistical analysis

All graphs and statistics (one-way ANOVA followed by Dunnet's multiple comparison test and two-way ANOVA for group comparison) were performed using GraphPad Prism® software (GraphPad Software, Inc., USA). Results represent mean ± S.E.M. and p values <0.05 were considered statistically significant.

3. Results

3.1. Effect of A_1 adenosine receptor activation on TG2-mediatedbiotin-cadaverine incorporation and protein cross-linking activity

Initial experiments investigated the effect of the selective A_1 adenosine receptor agonist CPA and the endogenous agonist adenosine on TG2 activity in H9c2 cardiomyoblasts. TGs can catalyse two types of cross-linking, namely (i) intra-, and/or inter-molecular covalent cross-links between protein-bound glutamine and protein-bound lysine residues, and (ii) cross-links between primary amines and protein-bound glutamine (both protein and polyamines links are transamidation).H9c2 cells were treated with CPA (1 μM) or adenosine (100 μM) for varying time periods and cell lysates subjected to the biotin-cadaverine amine-incorporation assay [25]. Both CPA and adenosine produced transient increases in TG2 catalysed biotin-cadaverine incorporation activity peaking at 10 min (Figure 1). Furthermore, CPA ($p[EC_{50}]$ = 8.87 ± 0.17; n=6) and adenosine ($p[EC_{50}]$ = 6.90 ± 0.11; n=7) stimulated concentration-dependent increases in amine incorporation activity (Figure 1).

The effect of A_1 adenosine receptor activation on TG2-mediated protein cross-linking activity in H9c2 cells was also determined using the biotin-labeled peptide (biotin-TVQQEL) cross-linking assay [28]. CPA and adenosine triggered time-dependent increases in TG2-mediated protein cross-linking activity peaking at 10 min (Figure 2). CPA ($p[EC_{50}]$ = 8.61 ± 0.20; n=6) and adenosine ($p[EC_{50}]$ = 7.01 ± 0.14; n=6) also stimulated concentration-dependent increases in protein cross-linking activity (Figure 2). The A_1 adenosine receptor antagonist DPCPX (1 μM) blocked CPA and adenosine-induced stimulation of TG2-mediated biotin amine incorporation activity and protein cross-linking activity (Figure 3). It is important to note that CPA, adenosine and DPCPX had no significant effect on purified guinea pig liver TG2 activity (data not shown).

3.2. The effect of TG2 inhibitors on A_1 adenosine receptor induced TG2 activity

To confirm that TG2 is the isoform linked to A_1 adenosine receptor transglutaminase activity in H9c2 cardiomyocytes, two structurally different cell permeable TG2 specific inhibitors were tested; R283 (a small molecule; [34]) and Z-DON (peptide-based; [35]). H9c2 cells were pre-treated for 1 h with Z-DON (150 μM) or R283 (200 μM) prior to stimulation with CPA for 10 min. As shown in Figure 3, Z-DON and R283 completely blocked CPA-induced TG2 activity, confirming the involvement of TG2 in these cell signaling responses. Comparable results were obtained in experiments using adenosine (Figure 3). Although there was variation in the effects of TG2 inhibitors on basal TG2

activity similar inhibitory trends were observed but these were not always statistically significant. However, the A_1 adenosine receptor antagonist DPCPX caused no noticeable effect on basal TG2 activity. In contrast, agonist activated levels of TG2 activity were consistently inhibited by either receptor antagonist or TG2 inhibitors. It is interesting to note that the levels of TG2 activity in the presence of CPA and R283 in particular are consistently lower than basal TG2 activity in the presence R283 alone. This is consistent with the possibility that CPA-activated TG2 is more amenable to inhibition by R283.

3.3. The effect of pertussis toxin and protein kinase inhibitors on A_1 adenosine receptor-induced TG2 activity

Pre-treatment with pertussis toxin ($G_{i/o}$-protein blocker; 100 ng/ml for 16 h) completely abolished CPA and adenosine induced transglutaminase amine incorporation activity and protein cross-linking activity, confirming the involvement of $G_{i/o}$-proteins (Figure 4). As shown in Figure 4, PD 98950 (50 μM; MEK1/2 inhibitor) and Ro 31-8220 (10 μM; PKC inhibitor) completely blocked CPA and adenosine-induced TG2 activity suggesting the involvement of ERK1/2 and PKC. Since the A_1 adenosine receptor activates other protein kinases including PKB [12,15], p38 MAPK [13] and JNK1/2 [36], we explored their role in A_1 adenosine receptor-induced TG2 activation. Modulation of protein kinase activity following A_1 adenosine receptor activation was assessed by Western blotting using phospho-specific antibodies that recognise phosphorylated motifs within activated ERK1/2 (pTEpY), p38 MAPK (pTGpY), JNK1/2 (pTPpY) and PKB (S^{473}). As shown in Figure 5, CPA (100 nM for 10 min) stimulated significant increases in ERK1/2, p38 MAPK and JNK1/2 phosphorylation in H9c2 cells. However, no activation of PKB by CPA was observed (data not shown). Pre-treatment with SB 203580 (20 μM; p38 MAPK inhibitor) or SP 600125 (20 μM; JNK1/2 inhibitor) blocked CPA-induced activation of p38 MAPK and JNK1/2, respectively (Figure 5) and CPA-mediated TG2 activity (Figure 6). It is important to note that Ro 31-8220, PD 98059, SB 203580 and SP 600125 had no significant effect on purified guinea pig liver TG2 activity (data not shown). Overall these data suggest that TG2 activity is modulated in H9c2 cells by the A_1 adenosine receptor via a multi protein kinase dependent signalling pathway.

3.4. Phosphorylation of TG2 following A_1 adenosine receptor activation

The effect of A_1 adenosine receptor activation on the phosphorylation status of TG2 was monitored via immunoprecipitation of TG2 followed by SDS-PAGE and Western blot analysis using anti-phosphoserine and anti-phosphothreonine antibodies. CPA (100 nM) triggered a robust increase in the levels of TG2-associated phosphoserine and phosphothreonine (Figure 7 and 8). Pre-treatment with Ro 318220 (10 μM), PD 98059

(50 μM) and SP 600125 (20 μM) blocked CPA-induced TG2 phosphorylation, whereas SB 203580 (20 μM) had no significant effect (Figure 7 and 8).

3.5. Visualisation of *in situ* TG2 activity following CPA and adenosine treatment

Biotin-X-cadaverine, a cell penetrating primary amine, acts as the acyl-acceptor in intracellular TG2-mediated transamidating reactions and becomes incorporated into endogenous protein substrates of TG2, which can subsequently be visualised by reporters such FITC- and HRP- ExtrAvidin® [37]. H9c2 cells were pre-incubated with 1 mM biotin-X-cadaverine for 6 h at 37°C prior to treatment with CPA or adenosine for 1, 5, 10, 20, 30 and 40 min. After fixation and permeabilisation, intracellular proteins with covalently attached biotin-X-cadaverine were visualized using ExtrAvidin®-FITC. As shown in Figure 9, CPA (1 μM) and adenosine (100 μM) induced time dependent increases in the incorporation of biotin-X-cadaverine into endogenous protein substrates of TG2. These data are comparable to the transient time-dependent increases in TG2 activity observed *in vitro* (see Figure 1). Surprisingly, given the covalent nature of biotin-X-cadaverine incorporation, fluorescence staining returned to control levels after 30 min incubation with CPA or 40 min incubation with adenosine. CPA and adenosine-mediated biotin-X-cadaverine incorporation was also concentration dependent (Figure 10). To confirm the involvement of TG2 activation, cells were treated with the TG2 inhibitors Z-DON (150 μM) and R283 (200 μM) for 1 h prior to incubation with CPA (100 nM for 10 min). Pre-treatment of cells with Z-DON, R283, DPCPX and pertussis toxin resulted in the complete inhibition of CPA-mediated biotin-X-cadaverine incorporation into protein substrates (Figure 11). Finally, the *in situ* responses to CPA were attenuated by the protein kinase inhibitors Ro 318220, PD 98059, SB 203580 and SP 600125 (Figure 12). Data comparable to those displayed in Figures 11 and 12 were also obtained for adenosine (data not shown).

3.6. The role of Ca^{2+} in A_1 adenosine receptor induced TG2 activity

CPA (100 nM) triggered intracellular Ca^{2+} oscillations that were dependent upon extracellular Ca^{2+} (Figure 13). Furthermore, pertussis toxin (100 ng/ml for 16 h) and the A_1 adenosine receptor antagonist DPCPX (1 μM) blocked CPA-induced Ca^{2+} signalling (Figure 13). Since TG2 is a Ca^{2+}-dependent enzyme we examined the role of Ca^{2+} in A_1 adenosine receptor-induced TG2 activation. The role of extracellular Ca^{2+} was assessed by measuring TG2 responses in the absence of extracellular Ca^{2+} using nominally Ca^{2+}-free Hanks/HEPES buffer containing 0.1 mM EGTA. Removal of extracellular Ca^{2+} abolished CPA- and adenosine-induced TG2 activity (Figure 14). The *in situ* responses to CPA and adenosine were also attenuated by removal of extracellular Ca^{2+} (data not

shown). These observations suggest that A_1 adenosine receptor-induced TG2 activation is dependent upon the influx of extracellular Ca^{2+}.

3.7. Identification of biotin-cadaverine labelled protein substrates

To detect the protein substrates from CPA-and adenosine-treated cells, substrates in whole cell extracts were enriched using CaptAvidin™-agarose sedimentation beads, resolved by 4-15% SDS-PAGE, and visualised using Coomassie blue stain. Figure 15 shows that treatment for 10 min with CPA (100 nM) or adenosine (100 μM) increased the incorporation of biotin-X-cadaverine into several proteins of different molecular masses in H9c2 cells. As expected, the incorporation of biotin-X-cadaverine into TG2 protein substrates was inhibited by pre-treatment with Z-DON and R283 (Figure 15). In order to identify the protein substrates for TG2–mediated amine incorporation, proteins captured and eluted from CaptAvidin™-agarose sedimentation beads were analysed by SWATH-MS (Sequential Windowed Acquisition of All Theoretical Fragment Ion Mass Spectra; [32]). This recently developed technique enables quantification of mass spectrometry data and hence the data presented are shown as CPA-induced fold-changes in proteins eluted from CaptAvidin™-agarose compared to control unstimulated cells. SWATH analysis revealed increases in 21 novel TG2 protein substrates and two previously identified substrates (e.g. histone H4 and voltage-dependent anion-selective channel protein 1) in response to A_1 adenosine receptor activation in H9c2 cells (Table 1).

3.8. The role of TG2 in A_1 adenosine receptor-induced cell survival

Our previous studies have shown that TG2 is involved in cytoprotection triggered by PKA and PKC-dependent signalling pathways in H9c2 cells [27]. In the current study the role of TG2 in A_1 adenosine receptor-induced cell survival was assessed in H9c2 cells following exposure of cells to 8 h hypoxia (1% O_2) in glucose-free and serum-free medium. In agreement with Fretwell and Dickenson [17], pre-treatment with CPA (100 nM) significantly attenuated hypoxia-induced decrease in MTT reduction and elevated release of LDH (Figure 16). Treatment with DPCPX (1 μM) reversed CPA-induced protection, confirming the involvement of the A_1 adenosine receptor (data not shown). The TG2 inhibitors R283 (200 μM) and Z-DON (150 μM) reversed CPA-induced cytoprotection, suggesting a role for TG2 in A_1 adenosine receptor-induced cell survival (Figure 16).

4. Discussion

4.1. In vitro modulation of TG2 by the A_1 adenosine receptor

The A_1 adenosine receptor agonist CPA and the endogenous agonist adenosine triggered a time- and concentration-dependent increase in TG2 activity in H9c2 cells. Adenosine-mediated increases in TG2 activity were completely blocked by the A_1 adenosine receptor antagonist DPCPX, suggesting involvement of the A_1 adenosine receptor.

As previously indicated, very little is known regarding the regulation of TG2 enzymatic activity by GPCRs. Examples in the literature include muscarinic receptor-mediated increases in TG2 activity in SH-SY5Y cells [38] and 5-HT_{2A} receptor mediated transamidation (TG-catalyzed) of the small G-protein Rac1 in the rat A1A1v cells [39]. Zhang *et al.*, [38] measured *in situ* TG2 activity (polyamine incorporation) triggered by the muscarinic agonist carbachol, whereas Dai *et al.*, [39] reported TG2 catalysed incorporation of 5-hydroxytryptamine into Rac1. 5-HT_{2A} receptor-mediated incorporation of 5-HT into the small GTPases RhoA and Rab4 was also observed in platelets [40]. It was suggested that 5-HT_{2A} and muscarinic receptor-mediated release of Ca^{2+} from intracellular Ca^{2+} stores may be responsible for triggering TG transamidating activity [38,40]. Hence, to our knowledge, the current study is the first demonstration of GPCR-mediated stimulation of the protein cross-linking activity of TG2. Furthermore, since the A_1 adenosine receptor couples to $G_{i/o}$-proteins it would be of interest to establish if other $G_{i/o}$-protein coupled receptors stimulate TG2 activity in H9c2 cells. Since we have previously shown that H9c2 express functional $G_{i/o}$-coupled kappa-opioid receptors it will be of interest to determine whether this member of the opioid receptor family modulates TG2 activity [41].

4.2. Role of Ca^{2+} in A_1 adenosine receptor-mediated TG2 activation

Although coupled to $G_{i/o}$-proteins, the A_1 adenosine receptor directly stimulates inositol phospholipid hydrolysis through G-protein $\beta\gamma$ subunit-mediated activation of phospholipase C in DDT_1MF-2 cells [42,43]. In this study, CPA triggered an increase in intracellular Ca^{2+} which was characterized by pronounced Ca^{2+} oscillations. Responses to CPA were abolished following removal of extracellular Ca^{2+}, suggesting that A_1 adenosine receptor-induced TG2 activation is dependent upon extracellular Ca^{2+} influx. Previous studies have shown that the A_1 adenosine receptor promotes the release of intracellular Ca^{2+} stores in basal forebrain cholinergic neurons, human bronchial smooth muscle cells and the smooth muscle cell line DDT_1MF-2 [44-46]. However, it is notable that in H9c2 cells the observed A_1 adenosine receptor-induced intracellular Ca^{2+} oscillations are dependent upon extracellular Ca^{2+} suggesting the involvement of Ca^{2+} influx. At present

the mechanism(s) associated with A_1 adenosine receptor-induced Ca^{2+} influx in H9c2 cells are not established, however, it is unlikely that voltage-gated Ca^{2+} channels are involved since activation of the $G_{i/o}$-protein coupled A_1 adenosine receptor is generally associated with the inhibition of P/Q- and N-type voltage-dependent Ca^{2+} channels [47]. An alternative mechanism for A_1 adenosine receptor-induced Ca^{2+} influx is via store-operated Ca^{2+} channels. Interestingly, the A_1 adenosine receptor promotes receptor-operated Ca^{2+} entry in cardiomyocytes via a phospholipase C and PKC-dependent pathway [48]. Although beyond the scope of the present study, it would be of interest to investigate the mechanism(s) underlying A_1 adenosine receptor-induced Ca^{2+} influx in H9c2 cells.

4.3. Role of protein kinases in A_1 adenosine receptor-mediated TG2 activation

Although TG2 activity can be regulated by changes in intracellular [Ca^{2+}] there is growing evidence that TG activity can also be modulated by phosphorylation [7,8]. The broad spectrum PKC inhibitor Ro 31-8220 and the MEK1/2 inhibitor PD 98059 completely blocked CPA and adenosine-induced TG2 activity, suggesting prominent roles for PKC and ERK1/2. Although ERK1/2 has been implicated in modulating the cross-linking activity of TG1 [8] there are no reports suggesting a role for this protein kinase in TG2 regulation. It is interesting to note that ERK1/2 activation by the A_1 adenosine receptor is sensitive to PKC inhibition in both neonatal rat cardiomyocytes [14] and H9c2 cells (data not shown) and, therefore, the role of PKC in TG2 activation maybe up-stream of ERK1/2. In view of the possible role of ERK1/2, we also determined whether A_1 adenosine receptor-induced TG2 activity involves PKB, p38 MAPK and JNK1/2. Although we detected A_1 adenosine receptor-induced stimulation of p38 MAPK and JNK1/2, we did not observe PKB activation by CPA in H9c2 cells. The kinase inhibitors SB203580 and SP600125 attenuated CPA-induced TG2 activity in H9c2 cells, suggesting a role for p38 MAPK and JNK1/2, respectively in A_1 adenosine receptor-induced TG2 activation.

Although beyond the scope of the present study, it is relevant to consider the possible signalling pathways associated with A_1 adenosine receptor-induced PKC, JNK1/2 and ERK1/2 activation. Previous studies have shown that the A_1 adenosine receptor activation promotes the selective translocation of PKC-ε and PKC-δ to the plasma membrane in cardiac myocytes [16,49]. Furthermore of the five PKC isozymes expressed in H9c2 cells (PKC-α, PKC-β_1, PKC-δ, PKC-ε, and PKC-ζ) adenosine stimulates the nuclear translation of PKC-ε [50]. Since DAG activates PKC-δ and PKC-ε, it is conceivable that the $G_{i/o}$-protein coupled A_1 adenosine receptor promotes PKC-δ/ε activation via G-protein $\beta\gamma$ subunit-mediated stimulation of phospholipase C [42,43,46]. It would be of interest in future studies to determine the PKC isozyme(s) involved in A_1 adenosine receptor-induced TG2 activation. At present, the signalling pathway(s) associated with A_1

adenosine receptor-induced ERK1/2 and JNK1/2 activation are not fully understood. The activation of ERK1/2 and JNK1/2 via $G_{i/o}$-PCRs is complex, involving both G protein α_i and $\beta\gamma$ subunit-dependent pathways (for a comprehensive review see [51]). Stimulation of JNK1/2 involves monomeric G-protein (e.g. Rac/Rho/Cdc42) mediated activation of MKK4/7, upstream kinases associated with JNK1/2 stimulation [51]. In contrast, $G_{i/o}$-PCR-mediated ERK1/2 activation involves PI-3K-dependent activation of Ras [51]. Indeed, our previous studies have shown that A_1 adenosine receptor-induced ERK1/2 activation in DDT_1MF-2 smooth muscle cells is dependent upon PI-3K activation [13]. Whether, some of the upstream kinases associated with the A_1 adenosine receptor-induced activation of JNK1/2 and ERK1/2 are also involved in modulating TG2 activity remains to be determined. Overall, it would seem that the A_1 adenosine receptor regulates TG2 activity in H9c2 cells via a multi-protein kinase dependent pathway. Although protein kinase inhibition and removal of extracellular Ca^{2+} both inhibit CPA-induced TG2 activity, the relationship between the two is not yet known.

4.4. A_1 adenosine receptor-induced phosphorylation of TG2

Given the apparent role of multiple serine/threonine kinases in the regulation of TG2 we investigated whether activation of the A_1 adenosine receptor results in the phosphorylation of TG2. The data presented demonstrate that TG2 is phosphorylated in response to A_1 adenosine receptor activation. To our knowledge, this represents the first report of enhanced TG2 phosphorylation in response to an exogenous stimulus. Previous studies have shown that TG2 is phosphorylated by PKA at Ser^{215} and Ser^{216} [52] and at an unknown site(s) by PTEN-induced putative kinase 1 (PINK1; [53]). Phosphoproteomic based studies have identified numerous phosphorylation sites on Ser, Thr and Tyr residues in human and rat TG2 [54-60]. It would therefore be of value to identify the specific site(s) of TG2-associated serine and threonine phosphorylation triggered by the A_1 adenosine receptor. It is interesting to note that PKA-mediated phosphorylation of TG2 has several consequences, including enhancement of protein-protein interactions and TG2 kinase activity [7,52], whereas PINK1-mediated phosphorylation of TG2 blocks its proteasomal degradation [53]. Thus, further studies are warranted in order to determine the functional consequence(s) of A_1 adenosine receptor-induced TG2 phosphorylation. In view of the multiple protein kinases implicated in A_1 adenosine receptor-induced TG2 activation, we investigated the influence of protein kinase inhibitors on TG2 phosphorylation. Although TG2 phosphorylation following A_1 adenosine receptor activation was attenuated by PKC, ERK1/2 and JNK1/2 inhibitors, further studies are needed to confirm if these protein kinases directly catalyse the phosphorylation of TG2. It is notable that the p38 MAPK inhibitor SB203580 did not

attenuate TG2 phosphorylation despite this kinase inhibitor blocking CPA-induced TG2 activity, suggesting that p38 MAPK modulates other targets involved in TG2 activation.

4.5. In situ modulation of TG2 activity and detection of TG2 protein substrates

Measurements of *in situ* TG2 activity following A_1 adenosine receptor stimulation were comparable to CPA- and adenosine-induced amine incorporation activity observed *in vitro*. However, given the covalent nature of biotin-X-cadaverine incorporation into protein substrates, it was surprising to observe that *in situ* TG2 activity returned to basal levels after 40 min. Possible explanations for this include reversal of amine incorporation catalysed by TG [61], that biotin-cadaverine labelled proteins were targeted for degradation or they were rapidly expelled from the cell. As we have previously reported the rapid expulsion of biotin-cadaverine labelled proteins from PMA- or forskolin-stimulated H9c2 cells [27], a similar mechanism may be responsible for the loss of biotinylated proteins following A_1 adenosine receptor activation.

SWATH™-MS analysis identified 21 novel TG2 protein substrates and two previously identified substrates (Table 1). Several of these proteins are associated with regulation of the cytoskeleton, transcription/translation, cell signaling and apoptosis, which supports the cytoprotective role for TG2 (see below). For example, hexokinase 1 (HK1) and acidic leucine-rich nuclear phosphoprotein 32 family member A (ANP32A) both exhibited in excess of 5-fold increases compared to the control. The former is a recognised as a mediator of cardioprotection via its interaction with mitochondrial voltage-dependent anion-selective channel protein 1 (VDAC1), which increased by over 2-fold in stimulated cells [62,63]. Interestingly, VDAC1 was previously identified as a TG2 substrate in PMA-stimulated H9c2 cells [27]. It may be that TG2-mediated amine incorporation into HK1 and VDAC interferes with the ability of these proteins to interact with each other and modulate cardioprotection and/or cell survival [64]. It is also notable that ANP32A functions as an inhibitor of protein phosphatase 2A and thus may regulate ERK1/2 and PKC; therefore it is conceivable that its modification by TG2 interferes with signalling events associated with cell survival [65,66]. As very little is currently known about the functional effects of TG2-mediated amine incorporation, further work to study the role of this phenomenon in TG2-induced cell survival would be warranted.

4.6. Role of TG2 in A_1 adenosine receptor-induced cytoprotection

The A_1 adenosine receptor mediates cell survival in several cell types including cardiomyocytes and neuronal cells [67,68]. The current study shows for the first time that TG2 is involved cytoprotection triggered by the A_1 adenosine receptor. TG2 is known to interact with or modulate a number of signalling pathways associated with cell survival against hypoxia and glucose deprivation-induced cell death, including hypoxia

inducible factor 1β, NF-κB and PKB [69,70]. It is also notable that several of the identified TG2 protein substrates are associated with cell survival/apoptosis. Further studies are required to determine the mechanism(s) associated with the role of TG2 in A_1 adenosine receptor-induced cell survival.

In conclusion, our data has shown for the first time that TG2 activity is regulated by the A_1 adenosine receptor in H9c2 cells. Furthermore, inhibitors of PKC, ERK1/2, p38 MAPK and JNK1/2 attenuated CPA-induced TG2 activation, suggesting a role for these kinases. We have also shown that activation of the A_1 adenosine receptor promotes TG2 phosphorylation via the aforementioned protein kinases and that TG2 plays a role in cytoprotection induced by CPA. Work to understand further the molecular mechanism(s) underlying the activation of TG2 by the A_1 adenosine receptor is currently underway.

Acknowledgements

We would like to thank Gordon Arnott for help with confocal imaging, Dr Carl Nelson for assistance with the Ca^{2+} imaging experiments and Dr Amanda Miles for help with proteomic analysis.

Conflict of Interest

The authors state no conflict of interest.

Figure legends

Figure 1. Effect of the A_1 adenosine receptor agonists CPA and adenosine on TG2-mediated biotin cadaverine amine incorporation activity in H9c2 cells. Time course profiles for (A) CPA (1 μM) and (B) adenosine (100 μM). Concentration-response curves for (C) CPA and (D) adenosine in cells treated with agonist for 10 min. Following stimulation, cells were lysed with 0.1 M Tris buffer pH 8.0 containing protease and phosphatase inhibitors. Cell lysates were then subjected to the biotin-cadaverine amine incorporation assay. Data points represent the mean ± S.E.M for TG2 specific activity from four to seven independent experiments. *P<0.05, **P<0.01, ***P<0.001, and ****P<0.0001 *versus* control response.

Figure 2. Effect of the A_1 adenosine receptor agonists CPA and adenosine on TG2-mediated peptide cross-linking activity in H9c2 cells. Time course profiles for (A) CPA (1 μM) and (B) adenosine (100 μM). Concentration-response curves for (C) CPA and (D) adenosine in cells treated with agonist for 10 min. Following stimulation, cells were lysed with 0.1 M Tris buffer pH 8.0 containing protease and phosphatase inhibitors. Cell lysates were then subjected to the peptide cross-linking assay. Data points represent the mean ± S.E.M for TG2 specific activity from four to six independent experiments. *P<0.05, **P<0.01, and ***P<0.001 *versus* control response.

Figure 3. Effect of the A_1 adenosine receptor antagonist DPCPX and TG2 inhibitors on CPA and adenosine-induced TG2 activity. H9c2 cells were pretreated for 30 min with the selective A_1 adenosine receptor antagonist DPCPX (1 μM) or for 1 h with the TG2 inhibitors Z-DON (150 μM) and R283 (200 μM) prior to 10 min stimulation with CPA (100 nM) or adenosine (100 μM). Cells were subsequently lysed with 0.1 M Tris buffer pH 8.0 containing protease and phosphatase inhibitors and cell lysates subjected to biotin cadaverine amine incorporation assay (panels A and B) or peptide cross-linking assay (panels C and D). Data points represent the mean ± S.E.M for TG2 specific activity from four independent experiments. *P<0.05, **P<0.01, ***P<0.001, and ****P<0.0001, (a) versus control and (b) versus 100 nM CPA or 100 μM adenosine alone.

Figure 4. Effect of the pertussis toxin and protein kinase inhibitors (for ERK1/2 and PKC) on A_1 adenosine receptor-induced TG2 activity. H9c2 cells were pretreated for 16 h with pertussis toxin (100 ng/ml) or for 30 min with PD98059 (50 μM) or Ro 31-8220 (10 μM)

prior to 10 min stimulation with CPA (100 nM) or adenosine (100 μM). Cells were subsequently lysed with 0.1 M Tris buffer pH 8.0 containing protease and phosphatase inhibitors and cell lysates subjected to biotin-cadaverine amine incorporation assay (panels A and B) or peptide cross-linking assay (panels C and D). Data points represent the mean ± S.E.M for TG2 specific activity from four independent experiments. *P<0.05, **P<0.01, ***P<0.001 and ****P<0.0001, (a) versus control and (b) versus 100 nM CPA or 100 μm adenosine alone.

Figure 5. Effect of the A_1 adenosine receptor agonist CPA on ERK1/2, p38 MAPK and JNK phosphorylation in H9c2 cells. Where indicated, H9c2 cells were pre-treated for 30 min with PD 98059 (50 μM), SB 203580 (20 μM) or SP 600125 (20 μM) prior to stimulation with CPA (100 nM) for 10 min. Cell lysates were analysed by Western blotting for activation of (A) ERK1/2, (B) p38 MAPK and (C) JNK using phospho-specific antibodies. Samples were subsequently analysed on separate blots using antibodies that recognize total ERK1/2, p38 MAPK and JNK. Data are expressed as the percentage of control cells (=100%) in the absence of protein kinase inhibitor and represent the mean ± S.E.M of four independent experiments. ***P<0.001, and ****P<0.0001, (a) versus control and (b) versus 100 nM CPA alone.

Figure 6. Effect of p38 MAPK and JNK1/2 inhibition on A_1 adenosine receptor-induced TG2 activity. H9c2 cells were pretreated for 30 min with SB 203580 (20 μM) or SP 600125 (20 μM) prior to 10 min stimulation with CPA (100 nM). Cells were subsequently lysed with 0.1 M Tris buffer pH 8.0 containing protease and phosphatase inhibitors and cell lysates subjected to biotin-cadaverine amine incorporation assay (panels A and B) or peptide cross-linking assay (panels C and D). Data points represent the mean ± S.E.M for TG specific activity from four independent experiments. *P<0.05, **P<0.01, ***P<0.001 and ****P<0.0001, (a) versus control and (b) versus 100 nM CPA alone.

Figure 7. Effect of PKC and ERK1/2 inhibitors on CPA-induced phosphorylation of TG2. Where indicated, H9c2 cells were pre-treated for 30 min with Ro 318220 (10 μM) or PD 98059 (50 μM) prior to stimulation with CPA (100 nM) for 10 min. Following stimulation with CPA, cell lysates were subjected immunoprecipitation using anti-TG2 monoclonal antibody as described in Materials and Methods. The resultant immunoprecipitated protein(s) were subjected to SDS-PAGE and analysed via Western blotting using (A)

anti-phosphoserine and (B) and anti-phosphothreonine antibodies. Samples were also analysed for TG2 levels. One tenth of the input was added to the first lane to show the presence of phosphorylated proteins prior to immunoprecipitation and negative controls with the immunoprecipitation performed only with beads or IgG were included to demonstrate the specificity of the bands shown. Quantified data for CPA-induced increases in TG2-associated serine and threonine phosphorylation are expressed as a percentage of that observed in control cells (100%). Data points represent the mean ± S.E.M from three independent experiments.*$P<0.05$, **$P<0.01$, and ***$P<0.001$, (a) versus control and (b) versus 100 nM CPA alone.

Figure 8. The effect of p38 MAPK and JNK1/2 inhibitors on CPA-induced phosphorylation of TG2. Where indicated, H9c2 cells were pre-treated for 30 min with SB 203580 (20 μM) or SP 600125 (20 μM) prior to stimulation with CPA (100 nM) for 10 min. Following stimulation with CPA, cell lysates were subjected immunoprecipitation using anti-TG2 monoclonal antibody as described in Materials and Methods. The resultant immunoprecipitated protein(s) were subjected to SDS-PAGE and analysed via Western blotting using (A) anti-phosphoserine and (B) anti-phosphothreonine antibodies. Samples were also analysed for TG2 levels. One tenth of the input was added to the first lane to show the presence of phosphorylated proteins prior to immunoprecipitation and negative controls with the immunoprecipitation performed only with beads or IgG were included to demonstrate the specificity of the bands shown. Quantified data for CPA-induced increases in TG2-associated serine and threonine phosphorylation are expressed as a percentage of that observed in control cells (100%). Data points represent the mean ± S.E.M from three independent experiments. *$P<0.05$, and **$P<0.01$, (a) versus control and (b) versus 100 nM CPA alone.

Figure 9. Time-dependent increases in *in situ*TG2 activity in H9c2 cells following stimulation with CPA and adenosine. Cells were incubated with 1 mM biotin-X-cadaverine (BTC) for 6 h after which they were treated with (A) 1 μM CPA or (B)100 μM adenosinefor 1, 5, 10, 20, 30 or 40 min. TG2-mediated biotin-X-cadaverine incorporation into intracellular proteins was visualized using FITC-conjugated ExtrAvidin® (green). Nuclei were stained with DAPI (blue) and viewed using a Leica TCS SP5 II confocal microscope (20x objective lens). Images presented are from one experiment and representative of three. Quantified data points for CPA (C) and adenosine (D) represent the mean ± S.E.M of fluorescence intensity per cell for five fields of view each from three

independent experiments. *P<0.05, **P<0.01, ***P<0.001 and ****P<0.0001 versus control response.

Figure 10. Concentration-dependent increases in *in situ* TG2 activity in H9c2 cells following stimulation with CPA and adenosine. Cells were incubated with 1 mM biotin-X-cadaverine (BTC) for 6 h after which they were treated with the indicated concentrations of (A) CPA or (B) adenosine for 10 min. TG2-mediated biotin-X-cadaverine incorporation into intracellular proteins was visualized using FITC-conjugated ExtrAvidin® (green). Nuclei were stained with DAPI (blue) and viewed using a Leica TCS SP5 II confocal microscope (20x objective lens). Images presented are from one experiment and representative of three. Quantified data points for CPA (C) and adenosine (D) represent the mean ± S.E.M of fluorescence intensity per cell for five fields of view each from four and three independent experiments, respectively. *P<0.05, **P<0.01, ***P<0.001 and ****P<0.0001 versus control response.

Figure 11. Effect of TG2 inhibitors, pertussis toxin and DPCPX on *in situ* TG2 activity in H9c2 cells following stimulation with CPA.(A) Cells were incubated with 1 mM biotin-X-cadaverine (BTC) for 6 h and then either treated for 1 h with the TG2 inhibitors Z-DON (150 μM) and R283 (200 μM), 16 h with pertussis toxin (100 ng/ml) or 30 min with DPCPX (1 μM) prior to 10 min stimulation with CPA (100 nM). TG2-mediated biotin-X-cadaverine incorporation into intracellular proteins was visualized using FITC-conjugated ExtrAvidin® (green). Nuclei were stained with DAPI (blue) and viewed using a Leica TCS SP5 II confocal microscope (20x objective lens). Images presented are from one experiment and representative of three. (B) Quantified data points represent the mean ± S.E.M of fluorescence intensity per nuclei for five fields of view each from three independent experiments. ***P<0.001 and ****P<0.0001, (a) versus control and (b) versus 100 nM CPA alone.

Figure 12. Effect of protein kinase inhibitors on *in situ* TG2 activity in H9c2 cells following stimulation with CPA.(A) Cells were incubated with 1 mM biotin-X-cadaverine (BTC) for 6 h and then treated for 30 min with Ro 31-8220 (10 μM), PD98059 (50 μM), SB 203580 (20 μM) or SP 600 125 (20 μM) prior to 10 min stimulation with CPA (100 nM). TG2-mediated biotin-X-cadaverine incorporation into intracellular proteins was visualized using FITC-conjugated ExtrAvidin® (green). Nuclei were stained with DAPI

(blue) and viewed using a Leica TCS SP5 II confocal microscope (20x objective lens).Images presented are from one experiment and representative of three. (B) Quantified data points represent the mean ± S.E.M of fluorescence intensity per cell for five fields of view each from three independent experiments.***$P<0.001$ and ****$P<0.0001$, (a) versus control and (b) versus 100 nM CPA alone.

Figure 13.Effect of the A_1 adenosine receptor agonist CPA on $[Ca^{2+}]_i$ in H9c2 cells. A) Confocal imaging snapshots of CPA (100 nM)-induced Ca^{2+} oscillations in the presence of extracellular Ca^{2+} (1.3 mM). The panel letters (a-g) correspond to the time points shown in trace B. B) The A_1 adenosine receptor agonist CPA triggered pronounced Ca^{2+} oscillations in the presence of extracellular Ca^{2+} (1.3 mM). C) Oscillations induced by CPA were absent during experiments performed in nominally Ca^{2+}-free buffer and 0.1 mM EGTA. In these experiments, depletion of intracellular Ca^{2+} stores with thapsigargin (5 μM) was still evident. D) Responses to CPA in the presence of extracellular Ca^{2+} were abolished by the A_1 adenosine receptor antagonist DPCPX (1 μM) and (E) following treatment with pertussis toxin (100 ng/ml for 16 h). ATP (10 μM) was added where indicated as a positive control. Similar were results were obtained in three other experiments.

Figure 14. The role of extracellular Ca^{2+} in CPA- and adenosine-induced TG2 activation. H9c2 cells were stimulated for 10 min with CPA (100 nM) or adenosine (100 μM) either in the presence of extracellular Ca^{2+} (1.8 mM) or in its absence using nominally Ca^{2+}-free Hanks/HEPES buffer containing 0.1 mM EGTA. Cells were subsequently lysed with 0.1 M Tris buffer containing protease and phosphatase inhibitors and cell lysates subjected to biotin-cadaverine amine incorporation (panel A) or peptide cross-linking assays (panel B). Data points represent the mean ± S.E.M for TG specific activity from four independent experiments. **$P<0.01$, ***$P<0.001$ and ****$P<0.0001$, (a) versus control in presence of extracellular Ca^{2+} , (b) versus 100 nM CPA in the presence of extracellular Ca^{2+},(c) versus 100 μM adenosine in the presence of extracellular Ca^{2+}.

Figure 15. Detection of *in situ* TG2 activity and protein substrates in CPA- and adenosine-treated H9c2 cells. Cells were incubated with 1 mM biotin-X-cadaverine for 6 h, after which they were treated for 1 h with the TG2 inhibitors Z-DON (150 μM) or R283 (200 μM) before stimulation with CPA (100 nM) or adenosine (100 μM) for 10 min.

Biotin-cadaverine labelled proteins were enriched using CaptAvidin™ agarose sedimentation beads and eluted proteins subjected to SDS-PAGE on a 4-15% polyacrylamide gradient. (A) Coomassie blue staining of enriched biotin-cadaverine labelled proteins following SDS-PAGE. (B) Quantification of protein substrates detected using Coomassie blue staining. Densitometry of each lane (total protein) was carried out using Advanced Image Data Analyser software (Fuji; version 3.52) and data are expressed as a percentage of basal TG2 protein substrate levels. Values are means ± S.E.M. from three independent experiments. *P<0.05 and**P<0.01, (a) versus control response, (b) versus CPA alone and (c) versus adenosine alone.

Figure 16. The effects of the TG2 inhibitors Z-DON and R283 on CPA-induced cell survival. H9c2 cells were pre-treated for 1 h with the TG2 inhibitors Z-DON (150 μM) or R283 (200 μM) before the addition of the A_1 adenosine receptor agonist CPA (100 nM) for 10 min prior to 8 h hypoxia (1% O_2) or 8 h normoxia. Cell viability was assessed by measuring (A) the metabolic reduction of MTT by cellular dehydrogenases and (B) release of LDH into the culture medium. Data are expressed as a percentage of normoxia control cell values (100%) and represent the mean ± S.E.M. from four independent experiments each performed in (A) quadruplicate and (B) sextuplicate. *P<0.05, **P<0.01 and ****P<0.0001, (a) versus normoxia control, (b) versus hypoxia control (c) versus 100 nM CPA in the presence of hypoxia.

Table 1. Identification of TG2 protein substrates.

Protein Name	Uniprot Accession	Uniprot Name	Absolute Fold Change*
[a]*Acidic leucine-rich nuclear phosphoprotein 32 family member A*	P49911	AN32A_RAT	5.38
[b]*Hexokinase-1*	P05708	HXK1_RAT	5.16
[a]*Nischarin*	Q4G017	NISCH_RAT	4.50
[c]*Tropomyosin alpha-3 chain*	Q63610	TPM3_RAT	4.34
[d]*Activated RNA polymerase II transcriptional co-activator p15*	Q63396	TCP4_RAT	3.34
[d]*60S ribosomal protein L13*	P41123	RL13_RAT	3.10
[d]Histone H4	P62804	H4_RAT	2.76
[e]*Calcineurin B homologous protein 1*	P61023	CHP1_RAT	2.71
[f]*Myeloid-associated differentiation marker*	Q6VBQ5	MYADM_RAT	2.66
[c]*Nestin*	P21263	NEST_RAT	2.61
[d]*60S ribosomal protein L30*	P62890	RL30_RAT	2.57
[f]*Transmembrane protein 33*	Q9Z142	TMM33_RAT	2.49
[c]*Tubulin alpha-3 chain*	Q68FR8	TBA3_RAT	2.14
[f]*Homer protein homolog 3*	Q9Z2X5	HOME3_RAT	2.13
[g]Voltage-dependent anion-selective channel protein 1	Q9Z2L0	VDAC1_RAT	2.11
[d]*MIF4G domain-containing protein*	Q6AXU7	MI4GD_RAT	2.09
[f]*Serine/threonine-protein phosphatase 2A 65 kDa regulatory subunit A beta isoform*	Q4QQT4	2AAB_RAT	2.08
[a]*Phosphatidylinositol 4-kinase type 2-alpha*	Q99M64	P4K2A_RAT	2.02
[h]*Extended synaptotagmin-1*	Q9Z1X1	ESYT1_RAT	1.89
[i]*Dolichyl-diphosphooligosaccharide--protein glycosyltransferase subunit 2*	P25235	RPN2_RAT	1.85
[d]*Translation initiation factor eIF-2B subunit delta*	Q63186	EI2BD_RAT	1.78
[h]*Coatomer subunit delta*	Q66H80	COPD_RAT	1.74
[d]*Y-box-binding protein 3*	Q62764	YBOX3_RAT	1.66

H9c2 cells were pre-incubated with biotin-X-cadaverine prior to treatment with CPA (100 nM) and biotin-cadaverine labelled proteins were captured and analysed by SWATH MS. [*]Absolute fold change in CPA-treated samples versus control (n=4) were calculated using SCIEX OneOmics with parameters MLR weight > 0.15, confidence >60% algorithms used described by Lambert *et* al., [33]. Proposed novel TG2 targets not appearing in the TG2 substrate database [71] or identified by Yu *et al*. [72] are indicated in *italics*. Protein substrates are grouped according to their functions and/or cellular function as follows: [a]cell signalling; [b]metabolism; [c]cytoskeletal; [d]transciption/translation; [e]vesicular trafficking; [f]structural/scaffolding protein; [g]apoptosis; [h]lipid/protein transport; [i]protein glycosylation.

References

[1] Lorand l, Conrad SM (1984) Transglutaminases. Mol Cell Biochem 58: 9-35.

[2] Nurminskaya MV, Belkin AM (2012) Cellular functions of tissue transglutaminase. Int Rev Cell Mol Biol 294: 1-97.

[3] Piacentini M, D'Eletto M, Falasca L, Farrace MG, Rodolfo C (2011) Transglutaminase 2 at the crossroads of cell death and survival. Adv Enzymol Relat Areas Mol Biol 78: 197-246.

[4] Caccamo D, Currò M, Lentile R (2010) Potential of transglutaminase 2 as a therapeutic target. Expert Opin Ther Targets 14: 989-1003.

[5] Gundemir S, Colak G, Tucholski J, Johnson GVW (2012) Transglutaminase 2: a molecular Swiss army knife. Biochim Biophys Acta 1823: 406-419.

[6] Mhaouty-Kodja S (2004) Ghα/tissue transglutaminase 2: an emerging G protein in signal transduction. Biol Cell 96: 363-367.

[7] Mishra S, Melino G, Murphy LJ (2007) Transglutaminase 2 kinase activity facilitates protein kinase A-induced phosphorylation of retinoblastoma protein. J Biol Chem 282: 18108-18115.

[8] Bollag WB, Zhong X, Dodd EM, Hardy DM, Zheng X, Allred WT (2005) Phospholipase D signaling and extracellular signal-regulated kinase-1 and -2 phosphorylation (activation) are required for maximal phorbol-ester-induced transglutaminase activity, a marker of keratinocyte differentiation. J Pharmacol Expt Ther 312: 1223-1231.

[9] Akar U, Ozpolat B, Mehta K, Fok J, Kondo Y, Lopez-Berestein G (2007) Tissue transglutaminase inhibits autophagy in pancreatic cancer cells. Mol Cancer Res 5: 241-249.

[10] Sheth S, Brito R, Mukherjea D, Rybak LP, Ramkumar V (2014) Adenosine receptors: expression, function and regulation. Int J Mol Sci 15: 2024-2052.

[11] Dickenson JM, Blank JL, Hill SJ (1998) Human adenosine A_1 receptor and $P2Y_2$-purinoceptor-mediated activation of the mitogen-activated protein kinase cascade in transfected CHO cells. Br J Pharmacol 124: 1491-1499.

[12] Germack R, Dickenson JM (2000) Activation of protein kinase B by the A_1 adenosine receptor in DDT_1MF-2 cells. Br J Pharmacol 130: 867-874.

[13] Robinson AJ, Dickenson JM (2001) Regulation of p42/p44 MAPK and p38 MAPK by the adenosine A_1 receptor in DDT_1MF-2 cells. Eur J Pharmacol 413: 151-161.

[14] Germack R, Dickenson JM (2004) Characterization of ERK1/2 signalling pathways induced by adenosine receptor subtypes in newborn rat cardiomyocytes. Br J Pharmacol 141: 329-339.

[15] Germack R, Griffin M, Dickenson JM (2005) Activation of protein kinase B by adenosine A_1 and A_3 receptors in newborn rat cardiomyocytes. J Mol Cell Cardiol 37: 989-999.

[16] Yang Z, Sun K, Hu K (2009) Adenosine A_1 receptors selectively target protein kinase C isoforms to the caveolin-rich plasma membrane in cardiac myocytes. Biochim Biophys Acta 1793: 1868-1875.

[17] Fretwell L, Dickenson JM (2009) Role of large-conductance Ca^{2+}-activated potassium channels in adenosine A_1 receptor-mediated pharmacological preconditioning in H9c2 cells. Eur J Pharmacol 618: 37-44.

[18] Kimes BW, Brandt BL (1976) Properties of a clonal muscle cell line from rat heart. Exp Cell Res 98: 367-381.

[19] Hescheler J, Meyer R, Plant S, Krautwurst D, Rosenthal W, Schultz G (1991) Morphological, biochemical and electrophysiological characterization of a clonal cell (H9c2) line from rat heart. Circ Res 69: 1476-1486.

[20] Davies PD, Hill CH, Keech E, Lawton G, Nixon JS, Sedgwick AD *et al*. (1989) Potent selective inhibitors of protein kinase C. FEBS Lett 259: 61-63.

[21] Dudley, DT, Pang L, Decker SJ, Bridges AJ, Saltiel AR (1995) A synthetic inhibitor of the mitogen-activated protein kinase cascade. Proc Natl Acad Sci USA 92: 7686-7689.

[22] Davies SP, Reddy H, Caivano M, Cohen P (2000) Specificity and mechanism of action of some commonly used protein kinase inhibitors. Biochem J 351: 95-105.

[23] Bennett BL, Sasaki DT, Murray BW, O'Leary EC, Sakata ST, Xu W *et al*. (2001) SP 600125, an anthrapyrazolone inhibitor of Jun N-terminal kinase. Proc Natl Acad Sci USA 98: 13681-13686.

[24] Smith PK, Krohn RI, Hermanson GT, Mallia AK, Gartner FH, Provenzano MD *et al. (*1985) Measurement of protein using bicinchoninic acid. Anal Biochem 150:76-85.

[25] Slaughter TF, Achyuthan KE, Lai TS, Greenberg CS (1992) A microtiter plate transglutaminase assay utilizing 5-(biotinamido) pentylamine as substrate. Anal Biochem 205: 166-171.

[26] Lilley GR, Skill J, Griffin M, Bonner PLR (1998) Detection of Ca^{2+}-dependent transglutaminase activity in root and leaf tissue of monocotyledonous and dicotyledonous plants. Plant Physiol 117: 1115-1123.

[27] Almami I, Dickenson JM, Hargreaves AJ, Bonner PLR (2014) Modulation of transglutaminase 2 activity in H9c2 cells by PKC and PKA signalling: a role for transglutaminase 2 in cytoprotection. Br J Pharmacol 171: 3946-3960.

[28] Trigwell SM, Lynch PT, Griffin M, Hargreaves AJ, Bonner PL (2004) An improved colorimetric assay for the measurement of transglutaminase (type II)-(γ-glutamyl) lysine cross-linking activity. Anal Biochem 330: 164-166.

[29] Mosmann T (1983) Rapid colorimetric assay for cellular growth and survival - application to proliferation and cyto-toxicity assays. J Immunol Meth 65: 55-63.

[30] Perry MJ, Mahoney SA, Haynes LW (1995) Transglutaminase C in cerebellar granule neurons: regulation and localization of substrate cross-linking. Neuroscience 65: 1063-1076.

[31] Singh RN, McQueen T, Mehta K (1995) Detection of the amine acceptor protein substrates of transglutaminase with 5-(biotinamido) pentylamine. Anal Biochem 231: 261-263.

[32] Huang Q, Yang L, Luo J, Guo L, Wang Z, Yang X *et al.* (2015) SWAH enables precise label-free quantification on proteome scale. Proteomics 15: 1215-1223.

[33] Lambert J-P, Ivosev G, Couzens AL, Larsen B, Taipale M, Lin Z-Y *et al*.(2013) Mapping differential interactomes by affinity purification coupled with data-independent mass spectrometry acquisition. Nature Meth 10: 1239-1245.

[34] Freund KF, Doshi KP, Gaul SL, Claremon DA, Remy DC, Baldwin JJ *et al*. (1994) Transglutaminase inhibition by 2-[(2-oxopropyl)thio]imidazolium derivatives: mechanism of factor XIIIa inactivation. Biochemistry 33: 10109-10119.

[35] Schaertl S, Prime M, Wityak J, Dominguez C, Munoz-Sanjuan I, Pacifici RE *et al.* (2010) A profiling platform for the characterization of transglutaminase 2 (TG2) inhibitors. J Biomol Screen 15: 478-487.

[36] Brust TB, Cayabyab FS, MacVicar BA (2007) C-Jun N-terminal kinase regulates adenosine A1 receptor-mediated synaptic depression in the rat hippocampus. Neuropharm 53: 906-917.

[37] Lee KN, Arnold SA, Birkbichler PJ, Patterson Jr MK, Fraij BM, Takeuchi Y, Carter HA (1993) Site-directed mutagenesis of human tissue transglutaminase: Cys-277 is essential for transglutaminase activity but not for GTPase activity. Biochim Biophys Acta 1202:1-6.

[38] Zhang J, Lesort M, Guttmann RP, Johnson GVW (1998) Modulation of the *in situ* activity of tissue transglutaminase by calcium and GTP. J Biol Chem 273: 2288-2295.

[39] Dai Y, Dudek NL, Patel TB, Muma NA (2008) Transglutaminase-catalysed transmidation: a novel mechanism for Rac1 activation by 5-hydroxytryptamine$_{2A}$ receptor stimulation. J Pharmacol Expt Ther 326: 153-162.

[40] Walther DJ, Peter J-U, Winter S, Höltje M, Paulmann N, Grohmann M *et al*. (2003) Serotonylation of small GTPases is a signal transduction pathway that triggers platelet α-granule release. Cell 115: 851-862.

[41] Dickenson JM, Fretwell L (2007) Functional expression of the adenosine A_1 and κ-opioid receptor in myocardiac H9c2 cells. Life Sciences 2007 Proc Life Sciences PC289.

[42] White TE, Dickenson JM, Alexander SPH, Hill SJ (1992) Adenosine A_1-receptor stimulation of inositol phospholipid hydrolysis and calcium mobilisation in DDT$_1$MF-2 cells. Br J Pharmacol 106: 215-221.

[43] Dickenson JM, Camps M, Gierschik P, Hill SJ (1995) Activation of phospholipase C by G-protein $\beta\gamma$ subunits in DDT$_1$MF-2 cells. Eur J Pharmacol 288: 393-398.

[44] Basheer R, Arrigoni E, Thatte HS, Greene RW, Ambudkar IS, McCarley RW (2002) Adenosine induces inositol 1,4,5-trisphosphate receptor-mediated mobilization of intracellular calcium stores in basal forebrain cholinergic neurons. J Neurosci 22: 7680-7686.

[45] Ethier MF, Madison JM (2006) Adenosine A_1 receptors mediate mobilization of calcium in human bronchial smooth muscle cells. Am J Respir Cell Mol Biol 35: 496-502.

[46] Dickenson JM, Hill SJ (1993) Adenosine A_1-receptor stimulated increases in intracellular calcium in the smooth muscle cell line DDT$_1$MF-2. Br J Pharmacol 108: 85-92.

[47] Gundlfinger A, Bischofberger J, Johenning FW, Torvinen M, Schmitz D Breustedt J (2007) Adenosine modulates transmission at the hippocampal mossy fibre synapse via direct inhibition of presynaptic calcium channels. J Physiol 582: 263-277.

[48] Sabourin J, Antigny F, Robin E, Frieden M, Raddatz E (2012) Activation of transient receptor potential canonical 3 (TRPC3)-mediated Ca^{2+} entry by A_1 adenosine receptor in cardiomyocytes disturbs atrioventricular conduction. J Biol Chem 287: 26688-26701.

[49] Henry P, Demolombe S, Pucéat M, Escande D (1996) Adenosine A_1 stimulation activates δ-protein kinase C in rat ventricular myocytes. Circ Res 78: 161-165.

[50] Xu TR, He G, Rumsby MG (2009) Adenosine triggers the nuclear translocation of protein kinase epsilon in H9c2 cardiomyoblasts with the loss of phosphorylation at Ser729. J Cell Biochem 106: 633-642.

[51] Goldsmith ZG, Dhanasekaran DN (2007) G protein regulation of MAPK networks. Oncogene 26: 3122-3142.

[52] Mishra S, Murphy LJ (2006) Phosphorylation of transglutaminase 2 by PKA at Ser216 creates 14.3.3 binding sites. Biochem Biophys Res Commun 347: 1166-1170.

[53] Min B, Kwon YC, Choe KM, Chung KC (2015) PINK1 phosphorylates transglutaminase 2 and blocks its proteasomal degradation. J Neurosci Res 93: 722-735.

[54] Hoffert JD, Pisitkun T, Wang G, Shen R-F, Knepper MA (2006) Quantitative phosphoproteomics of vasopressin-sensitive renal cells: regulation of aquaporin-2 phosphorylation at two sites. PNAS 103: 7159-7164.

[55] Rikova K, Guo A, Zeng Q, Possemato A, Yu J, Haack H *et al*. (2007) Global survey of phosphotyrosine signaling identifies oncogenic kinases in lung cancer. Cell 131: 1190-1203.

[56] Imami K, Sugiyama N, Kyono Y, Tomita M, Ishihama Y (2008) Automated phosphoproteome analysis for cultured cancer cells by two-dimensional nano LC-MS using a calcined titania/C18 biphasic column. Analyt Sci. 24: 161-166.

[57] Kettenbach AN, Schweppe DK, Faherty BK, Pechenick D, Pletnev AA, Gerber SA (2011) Quantitative phosphoproteomics identifies substrates and functional modules of Aurora and Polo-like kinase activities in mitotic cells. Sci Signal 4: rs5. doi: 10.1126/scisignal.2001497.

[58] Lundby A, Secher A, Lage K, Nordsborg NB, Dmytriyev A, Lundby C, Olsen JV (2012) Quantitative maps of protein phosphorylation sites across 14 different rat organs and tissues. Nature Commun 3:876 doi: 10.1038/ncomms1871.

[59] Bian Y, Song C, Cheng K, Dong M, Wang F, Huang J *et al*. (2014) An enzyme assisted RP-RPLC approach for in-depth analysis of human liver phosphoproteome. J Proteomics 96: 253-262.

[60] Palacios-Moreno J, Foltz L, Guo A, Stokes MP, Kuehn ED, George L *et al*. (2015) Neuroblastoma tyrosine kinase signaling networks involve FYN and LYN I endosomes and lipid rafts. PLoS Comput Biol 11(4): e1004130. doi: 10.1371/journal.pcbi.1004130

[61] Stamnaes J, Fleckenstein B, Sollid LM (2008) The propensity for deamidation and transamidation of peptides by transglutaminase 2 is dependent on substrate affinity and reaction conditions. Biochimica et Biophysica Acta 1784: 1804-1811.

[62] Calmettes G, Ribalet B, John S, Korge P, Ping P, Weiss JN (2015) Hexokinases and cardioprotection. J Mol Cell Cardiol 78: 107-115.

[63] Halestrap AP, Pereira GC, Pasdois P (2015) The role of hexokinase in cardioprotection- mechanism and potential for translation. Br J Pharmacol 172: 2085-2100.

[64] Keinan N, Tyomkin D, Shoshan-Barmatz V (2010) Oligomerization of the mitochondrial protein voltage-dependent anion channel is coupled to the induction of apoptosis. Mol Cell Biol 30: 5698-5709.

[65] Matilla A, Radrizzani M (2005) The Anp32 family of proteins containing leucine-rich repeats. Cerebellum 4: 7-18.

[66] Seshacharyulu P, Pandey P, Datta K, Batra SK (2013) Phosphatase: PP2A structural importance, regulation and its aberrant expression in cancer. Cancer Letts 335: 9-18.

[67] Di-Capua N, Sperling O, Zoref-Shani (2003) Protein kinase C-ε is involved in the adenosine-activated signal transduction pathway conferring protection against ischemia-reperfusion injury in primary rat neuronal cells. J Neurochem 84: 409-412.

[68] Germack R, Dickenson JM (2005) Adenosine triggers preconditioning through MEK/ERK1/2 signalling pathway during hypoxia/reoxygenation in neonatal rat cardiomyocytes. J Mol Cell Cardiol 39: 429-442.

[69] Filiano AJ, Bailey CDC, Tucholski J, Gundemir S, Johnson GVW (2008) Transglutaminase 2 protects against ischemic insult, interacts with HIF1β, and attenuates HIF1 signaling. FASEB J 22: 2662-2675.

[70] Wang Y, Ande SR, Mishra S (2012) Phosphorylation of transglutaminase 2 (TG2) at serine-216 has a role in TG2 mediated activation of nuclear factor-kappa B and in the downregulation of PTEN. BMC Cancer 12: 277.

[71] Csósz E, Meskó B, Fésüs L (2009) Transdab wiki: the interactive transglutaminase substrate database on web 2.0 surface. Amino Acids 36: 615-617.

[72] Yu C-H, Chou C-C, Lee Y-J, Khoo K-H, Chang G-D (2015) Uncovering protein polyamination by the spermine-specific antiserum and mass spectrometric analysis. Amino Acids 47: 469-481.

Figure 1

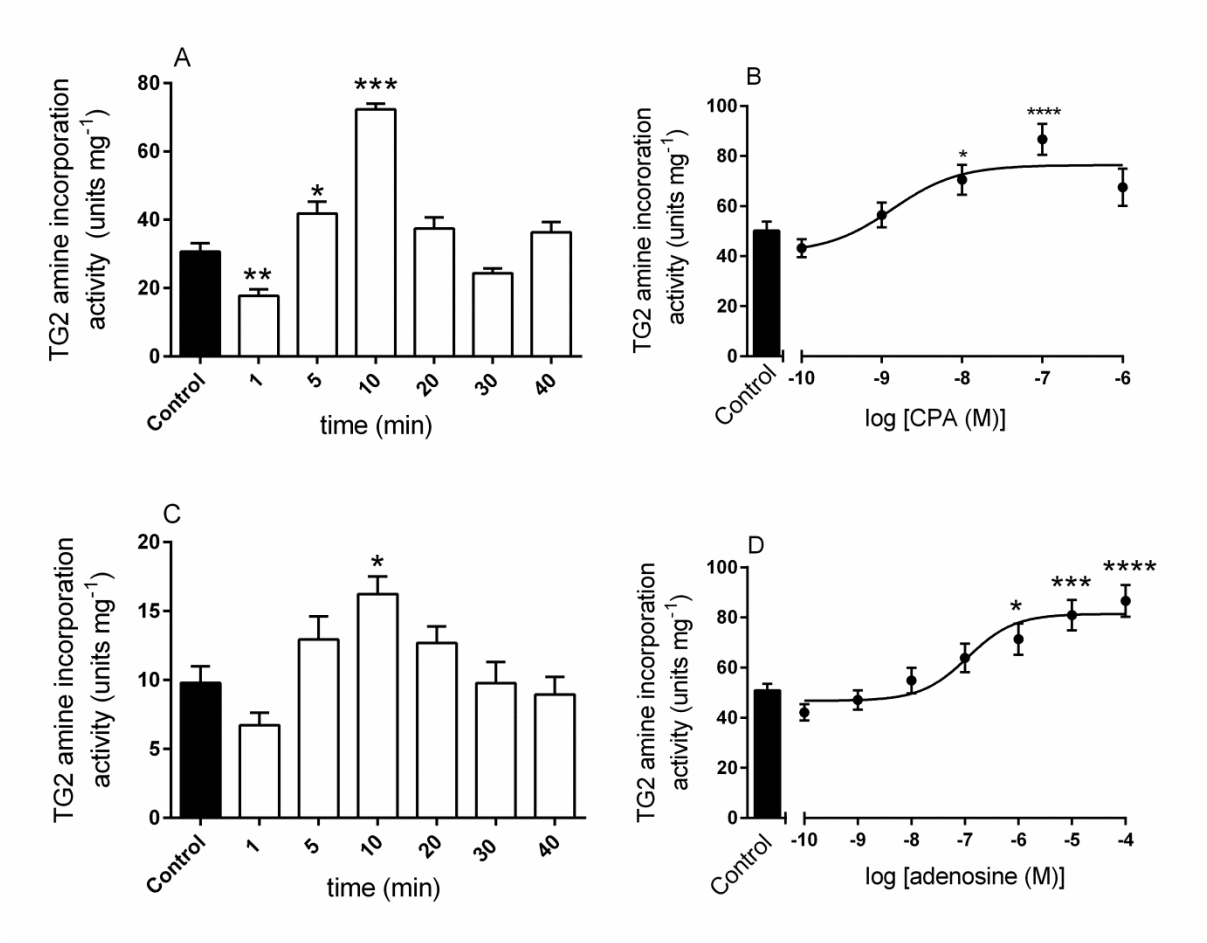
A
TG2 amine incorporation activity (units mg-1)
80
60
40
20
0
**
*
***
Control
1
5
10
20
30
40
time (min)
B
TG2 amine incororation activity (units mg-1)
100
80
60
40
20
0
*
****
Control
-10
-9
-8
-7
-6
log [CPA (M)]
C
TG2 amine incorporation activity (units mg-1)
20
15
10
5
0
*
Control
1
5
10
20
30
40
time (min)
D
TG2 amine incorporation activity (units mg-1)
100
80
60
40
20
0
*
***
****
Control
-10
-9
-8
-7
-6
-5
-4
log [adenosine (M)]

Figure 2

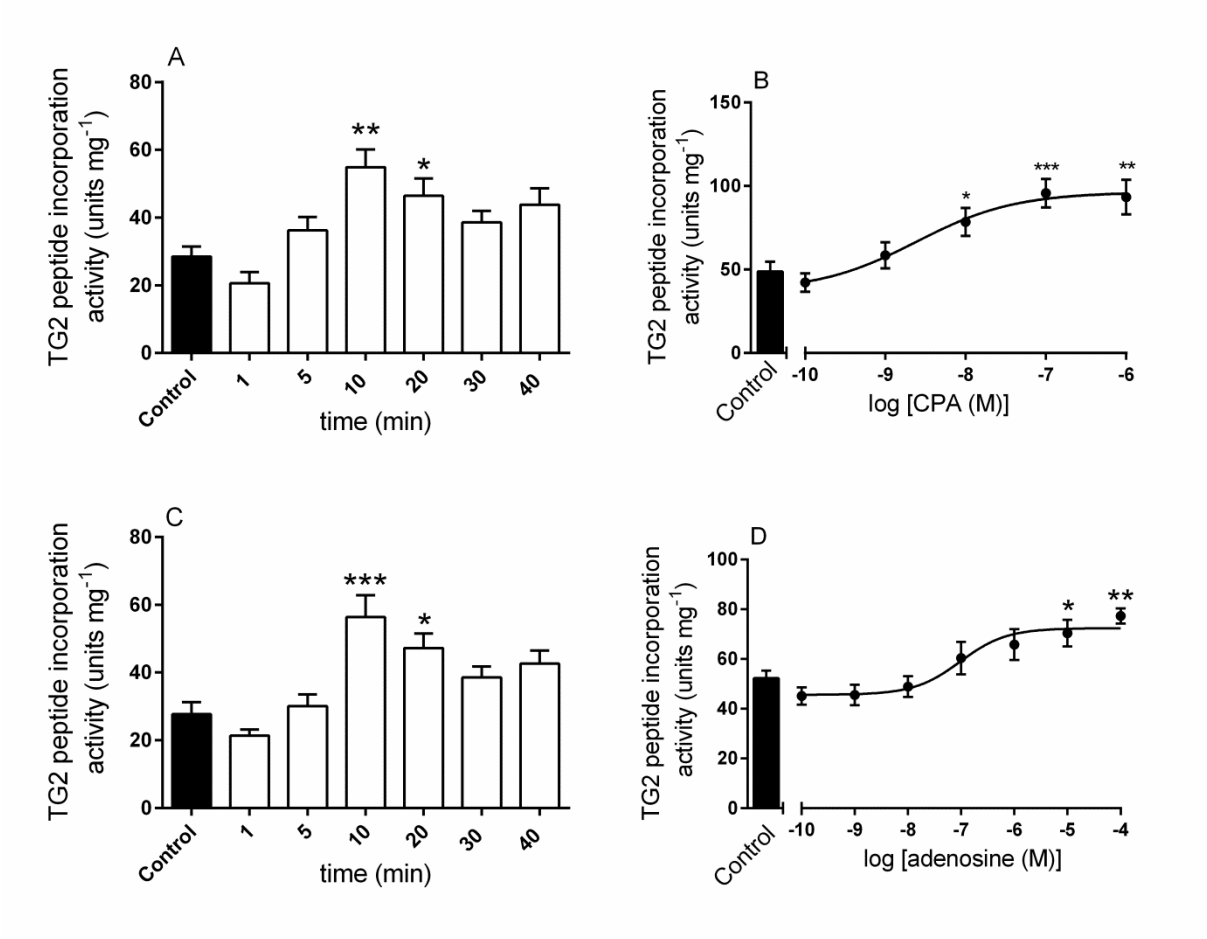
A
TG2 peptide incorporation activity (units mg-1)
80
60
40
20
0
**
*
Control
1
5
10
20
30
40
time (min)
B
TG2 peptide incorporation activity (units mg-1)
150
100
50
0
*
***
**
Control
-10
-9
-8
-7
-6
log [CPA (M)]
C
TG2 peptide incorporation activity (units mg-1)
80
60
40
20
0
***
*
Control
1
5
10
20
30
40
time (min)
D
TG2 peptide incorporation activity (units mg-1)
100
80
60
40
20
0
*
**
Control
-10
-9
-8
-7
-6
-5
-4
log [adenosine (M)]

Figure 3

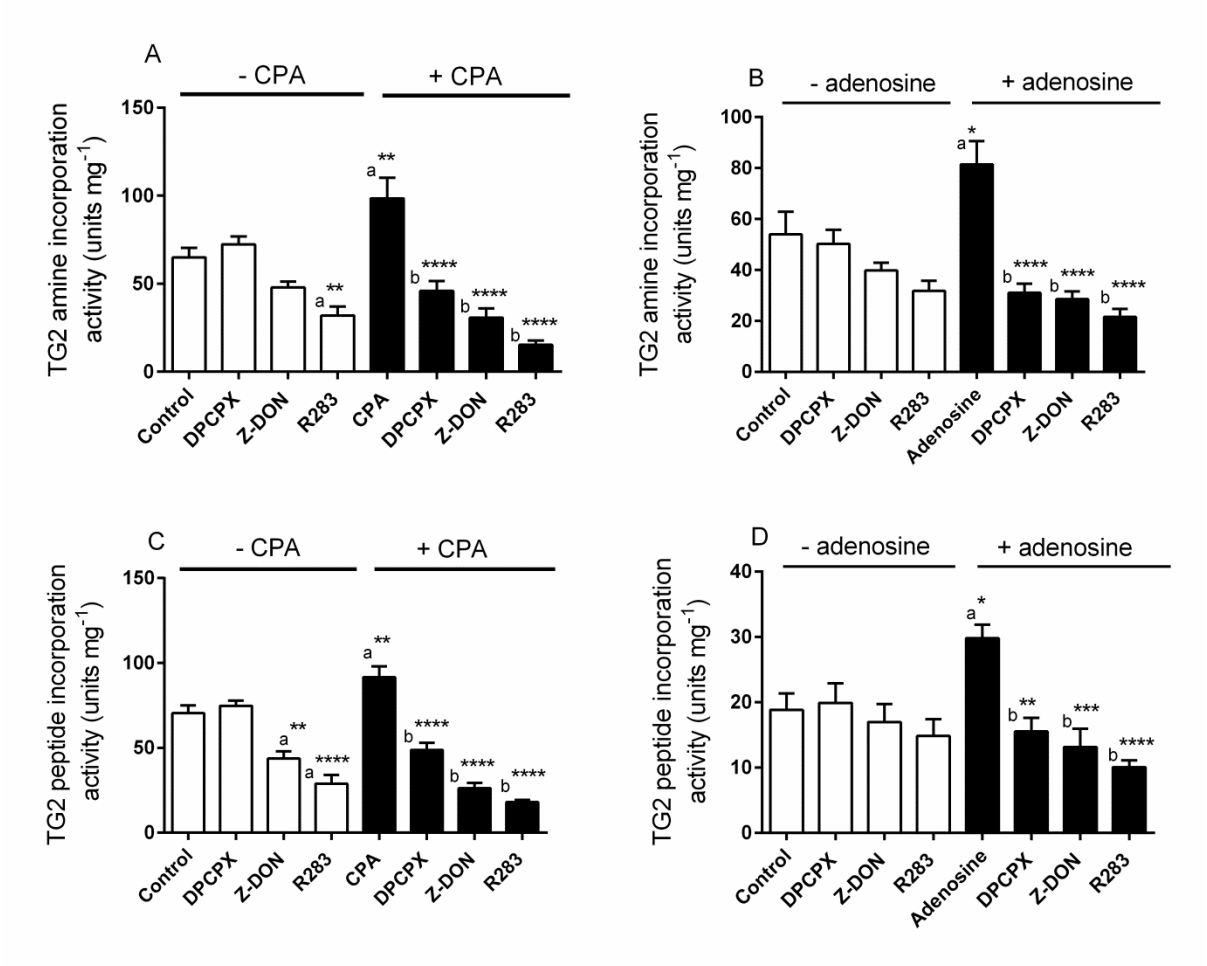
A
- CPA
+ CPA
TG2 amine incorporation activity (units mg-1)
150
100
50
0
Control
DPCPX
Z-DON
R283
CPA
DPCPX
Z-DON
R283
B
- adenosine
+ adenosine
TG2 amine incorporation activity (units mg-1)
100
80
60
40
20
0
Control
DPCPX
Z-DON
R283
Adenosine
DPCPX
Z-DON
R283
C
- CPA
+ CPA
TG2 peptide incorporation activity (units mg-1)
150
100
50
0
Control
DPCPX
Z-DON
R283
CPA
DPCPX
Z-DON
R283
D
- adenosine
+ adenosine
TG2 peptide incorporation activity (units mg-1)
40
30
20
10
0
Control
DPCPX
Z-DON
R283
Adenosine
DPCPX
Z-DON
R283

Figure 4

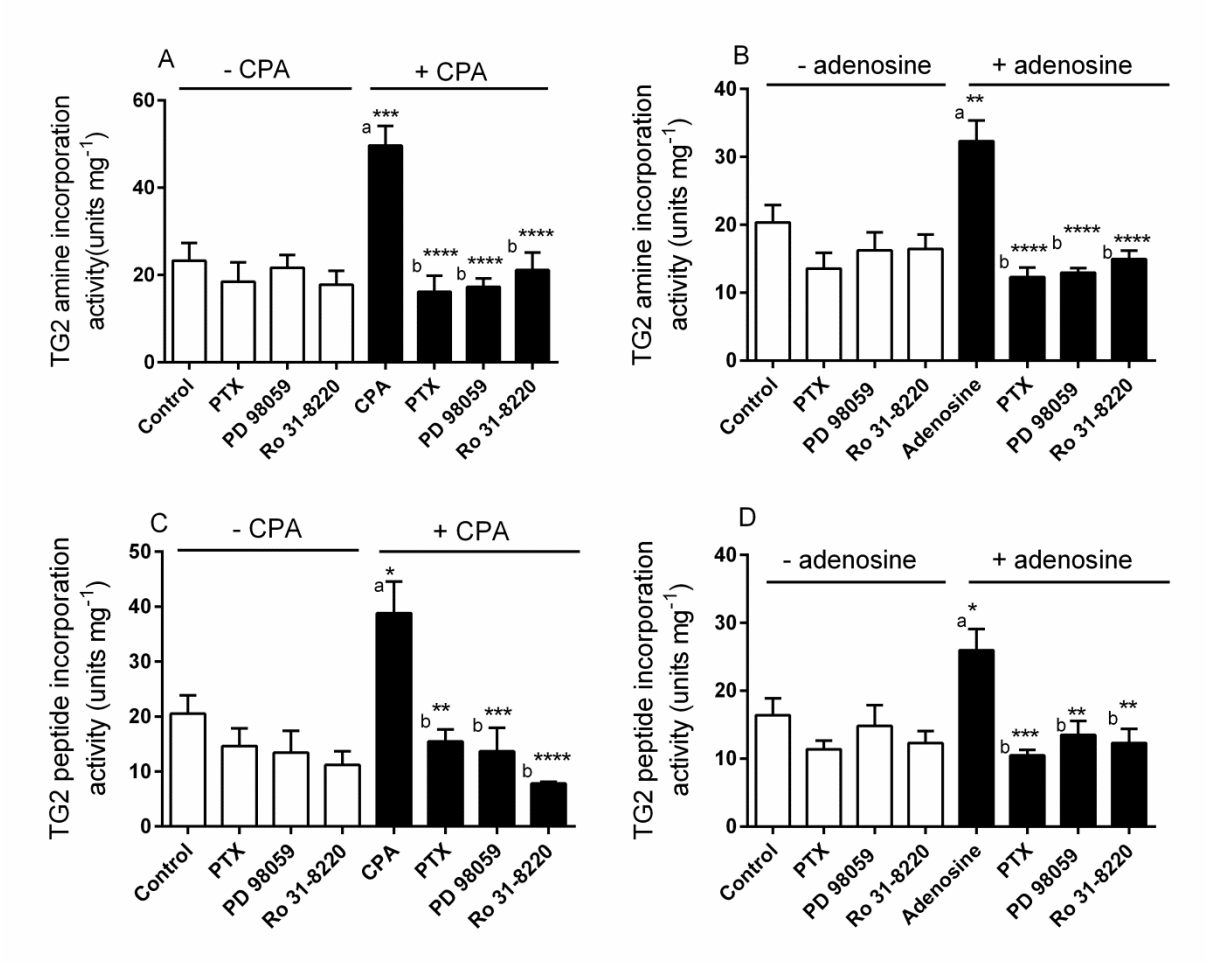
A
- CPA
+ CPA
TG2 amine incorporation activity(units mg-1)
Control
PTX
PD 98059
Ro 31-8220
CPA
B
- adenosine
+ adenosine
TG2 amine incorporation activity (units mg-1)
Adenosine
C
TG2 peptide incorporation activity (units mg-1)
D

Figure 5

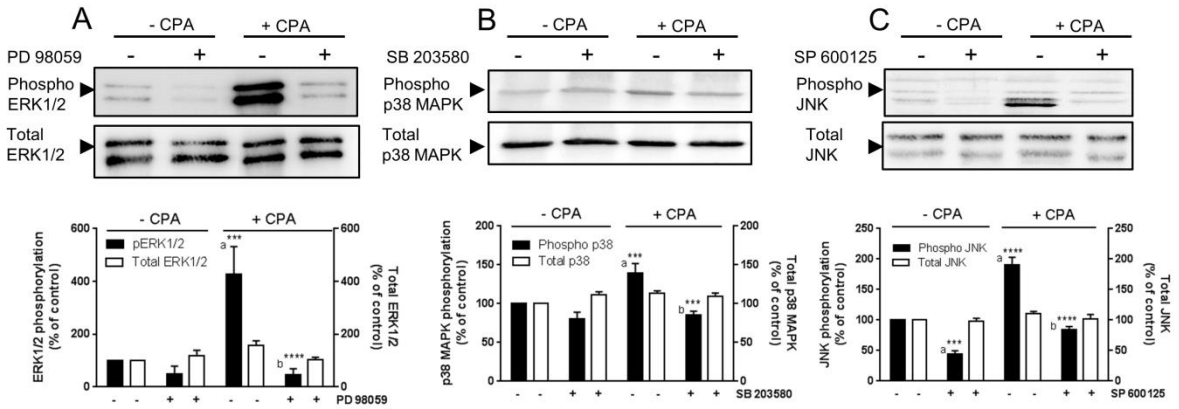
A
- CPA
+ CPA
PD 98059
Phospho ERK1/2
Total ERK1/2
B
SB 203580
Phospho p38 MAPK
Total p38 MAPK
C
SP 600125
Phospho JNK
Total JNK
pERK1/2
Total ERK1/2
ERK1/2 phosphorylation (% of control)
Total ERK1/2 (% of control)
Phospho p38
Total p38
p38 MAPK phosphorylation (% of control)
Total p38 MAPK (% of control)
Phospho JNK
Total JNK
JNK phosphorylation (% of control)
Total JNK (% of control)

Figure 6

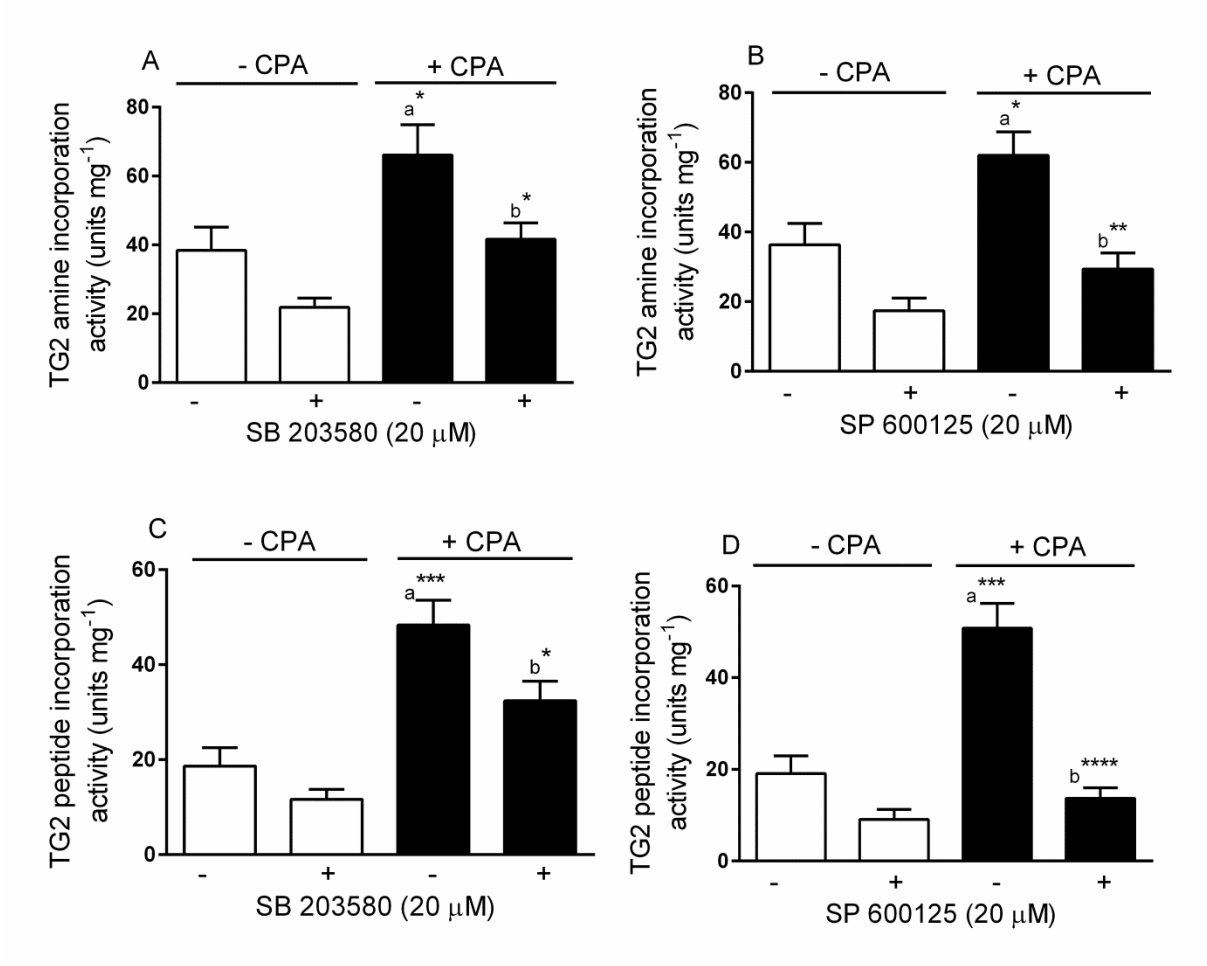
A
- CPA
+ CPA
TG2 amine incorporation activity (units mg-1)
SB 203580 (20 μM)
B
SP 600125 (20 μM)
C
TG2 peptide incorporation activity (units mg-1)
D

Figure 7

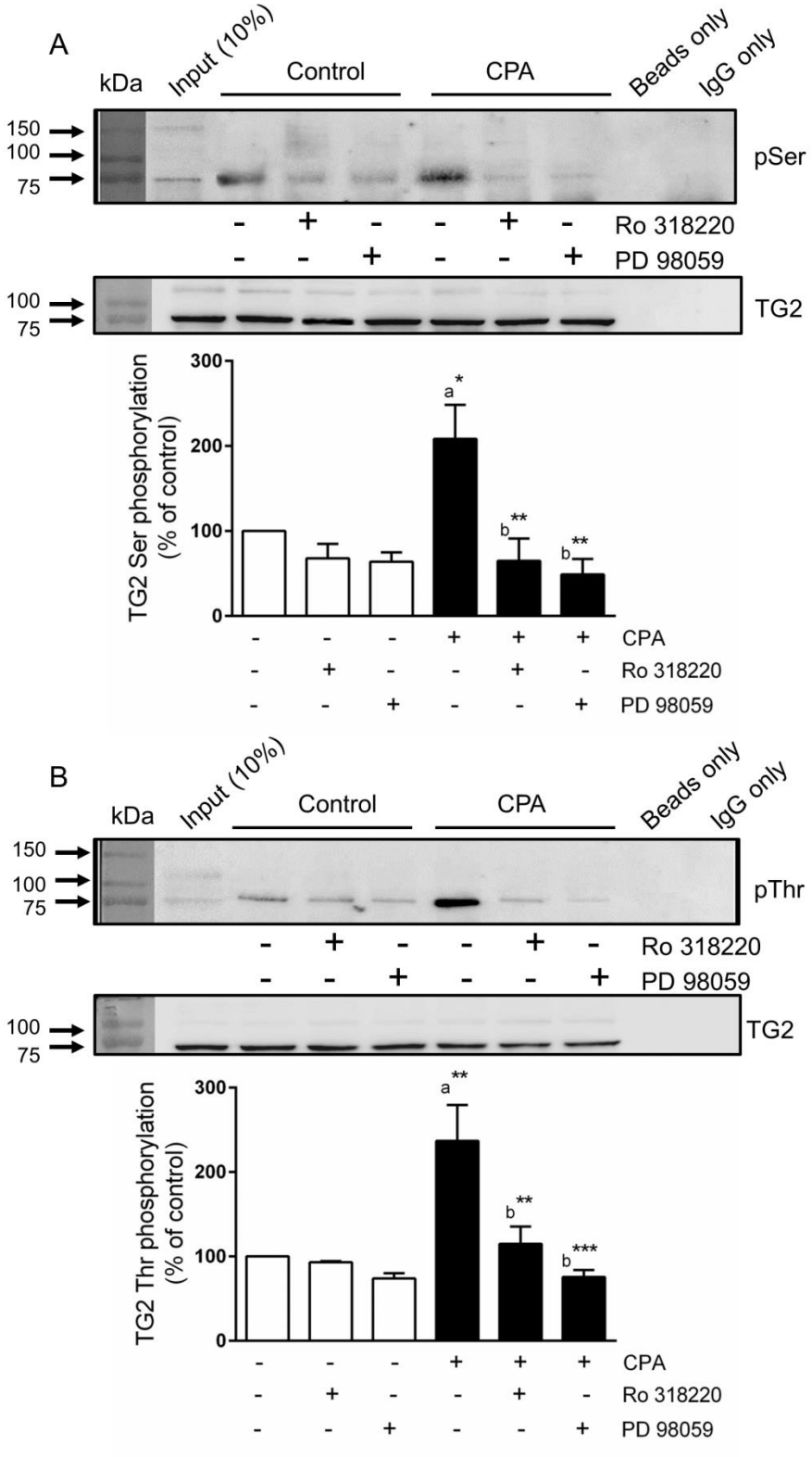
A
kDa
Input (10%)
Control
CPA
Beads only
IgG only
150
100
75
pSer
Ro 318220
PD 98059
100
75
TG2
TG2 Ser phosphorylation (% of control)
300
200
100
0
a *
b **
b **
CPA
Ro 318220
PD 98059
B
kDa
Input (10%)
Control
CPA
Beads only
IgG only
150
100
75
pThr
Ro 318220
PD 98059
100
75
TG2
TG2 Thr phosphorylation (% of control)
300
200
100
0
a **
b **
b ***
CPA
Ro 318220
PD 98059

Figure 8

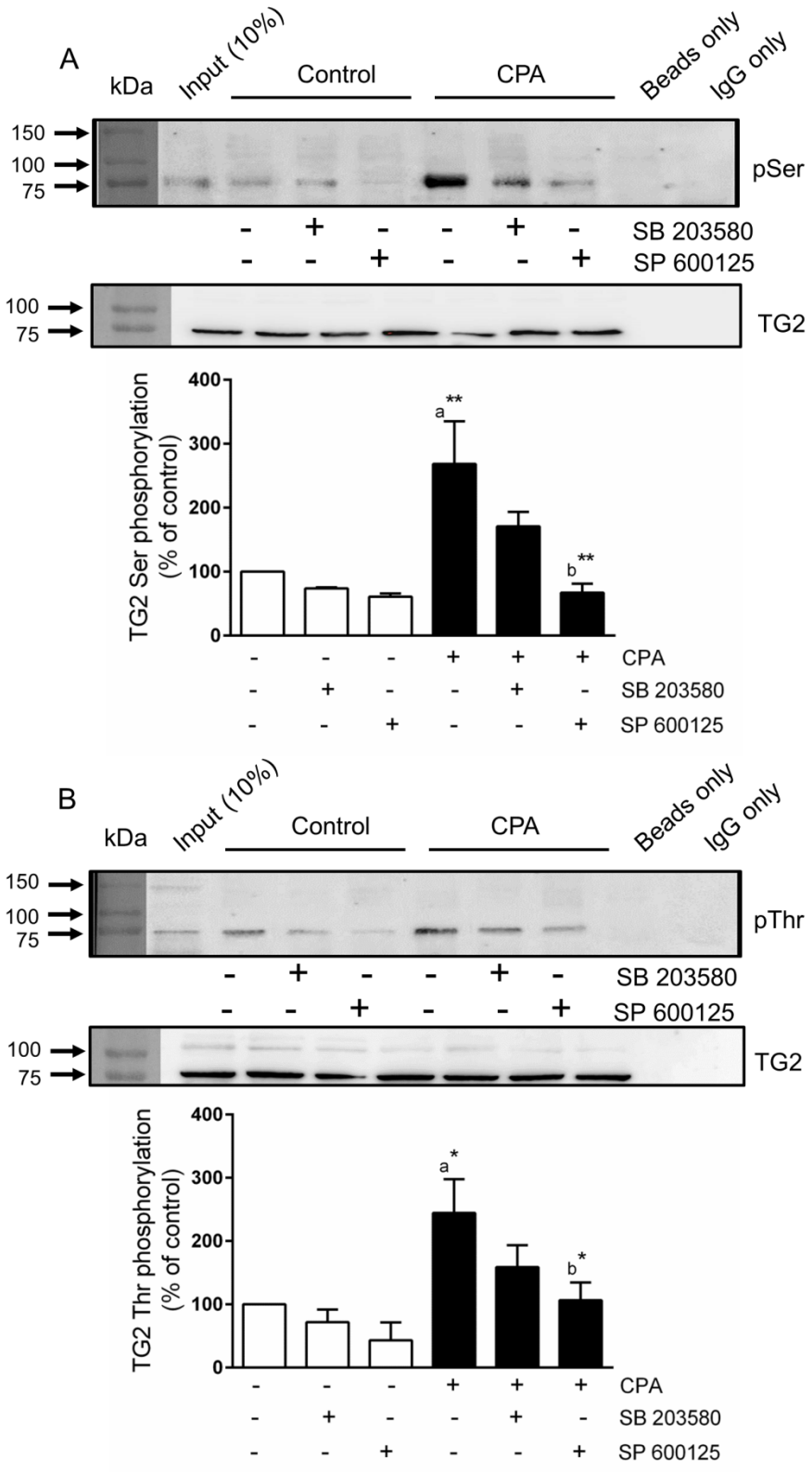
A
kDa
Input (10%)
Control
CPA
Beads only
IgG only
150
100
75
pSer
SB 203580
SP 600125
100
75
TG2
TG2 Ser phosphorylation (% of control)
400
300
200
100
0
a**
b**
CPA
SB 203580
SP 600125
B
kDa
Input (10%)
Control
CPA
Beads only
IgG only
150
100
75
pThr
SB 203580
SP 600125
100
75
TG2
TG2 Thr phosphorylation (% of control)
400
300
200
100
0
a*
b*
CPA
SB 203580
SP 600125

Figure 9

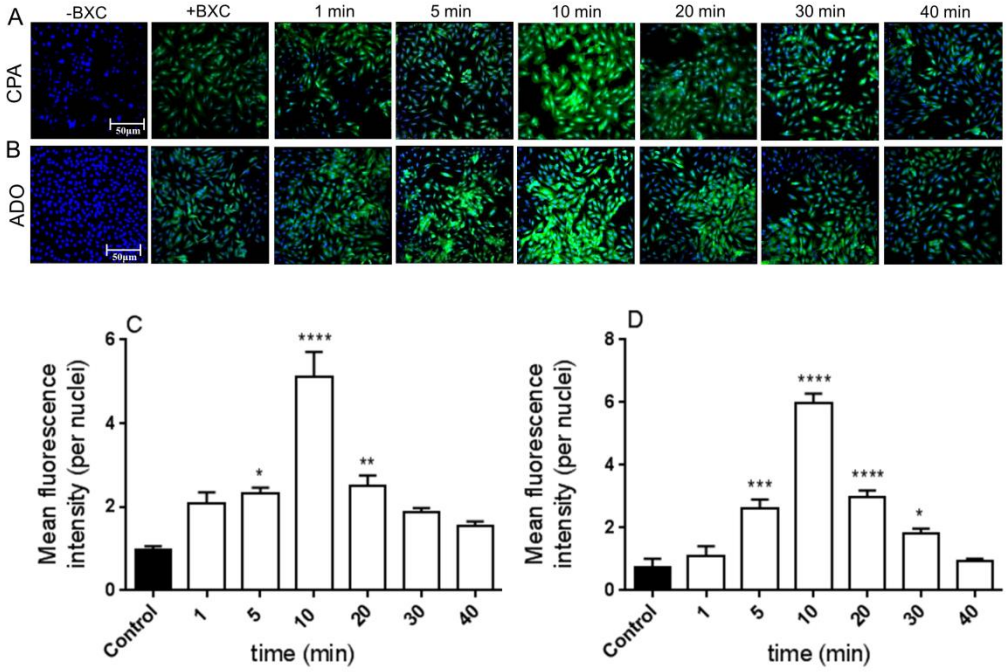
A
-BXC
+BXC
1 min
5 min
10 min
20 min
30 min
40 min
CPA
B
ADO
50µm
C
Mean fluorescence intensity (per nuclei)
time (min)
Control
D
Mean fluorescence intensity (per nuclei)
time (min)
Control

Figure 10

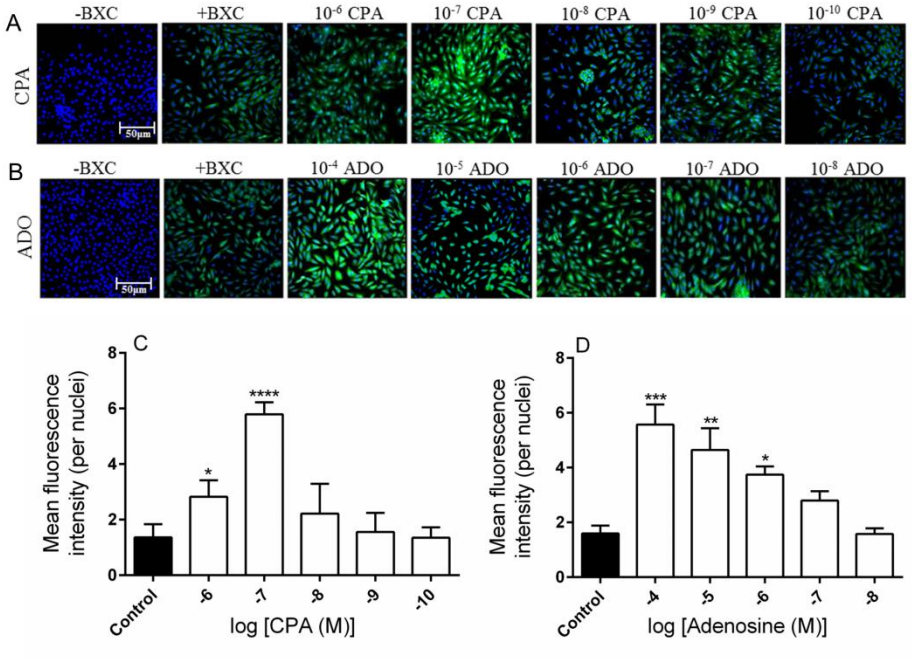
A
-BXC
+BXC
10-6 CPA
10-7 CPA
10-8 CPA
10-9 CPA
10-10 CPA
CPA
50µm
B
-BXC
+BXC
10-4 ADO
10-5 ADO
10-6 ADO
10-7 ADO
10-8 ADO
ADO
50µm
C
Mean fluorescence intensity (per nuclei)
Control
-6
-7
-8
-9
-10
log [CPA (M)]
D
Mean fluorescence intensity (per nuclei)
Control
-4
-5
-6
-7
-8
log [Adenosine (M)]

Figure 11

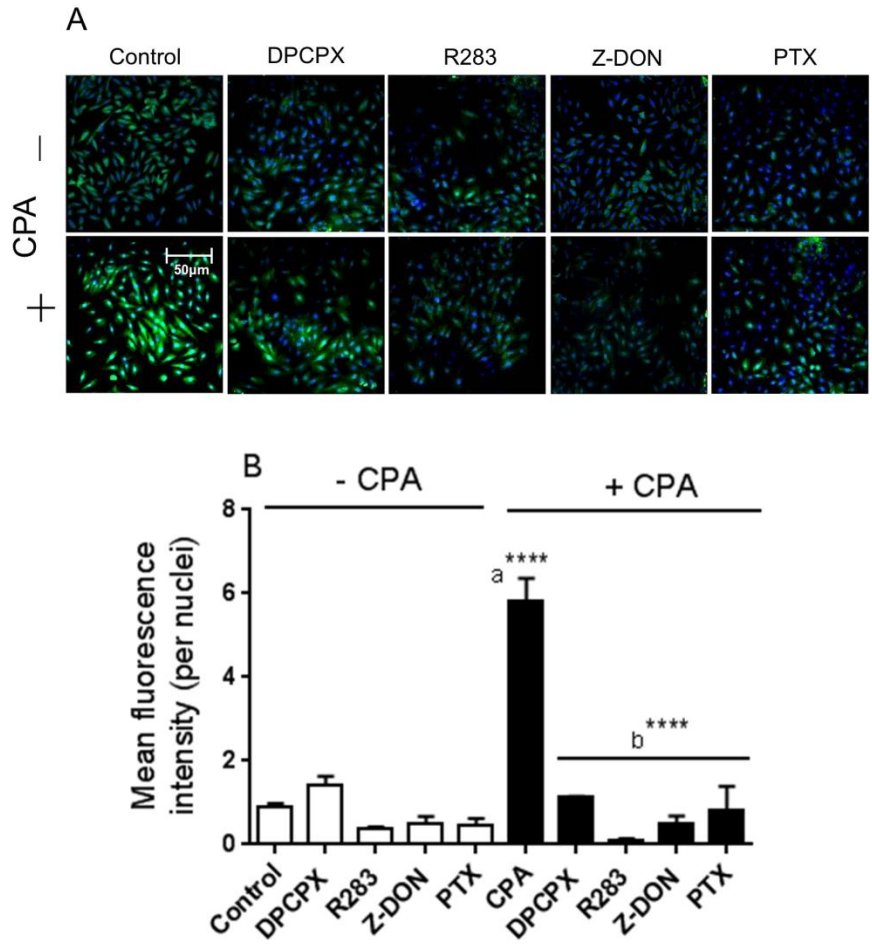
A
Control
DPCPX
R283
Z-DON
PTX
CPA
–
+
50µm
B
- CPA
+ CPA
Mean fluorescence intensity (per nuclei)
8
6
4
2
0
****
a
b
****
Control
DPCPX
R283
Z-DON
PTX
CPA
DPCPX
R283
Z-DON
PTX

Figure 12

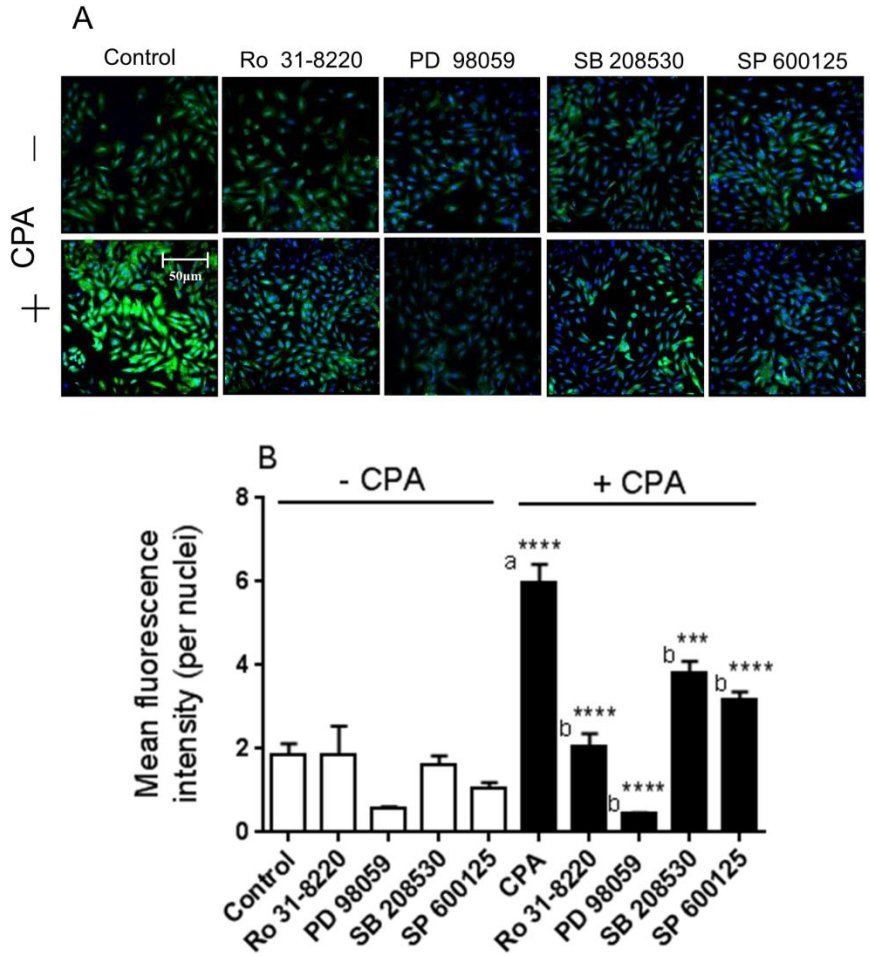
A
Control
Ro 31-8220
PD 98059
SB 208530
SP 600125
CPA
50µm
B
- CPA
+ CPA
Mean fluorescence intensity (per nuclei)
Control
Ro 31-8220
PD 98059
SB 208530
SP 600125
CPA
Ro 31-8220
PD 98059
SB 208530
SP 600125

Figure 13

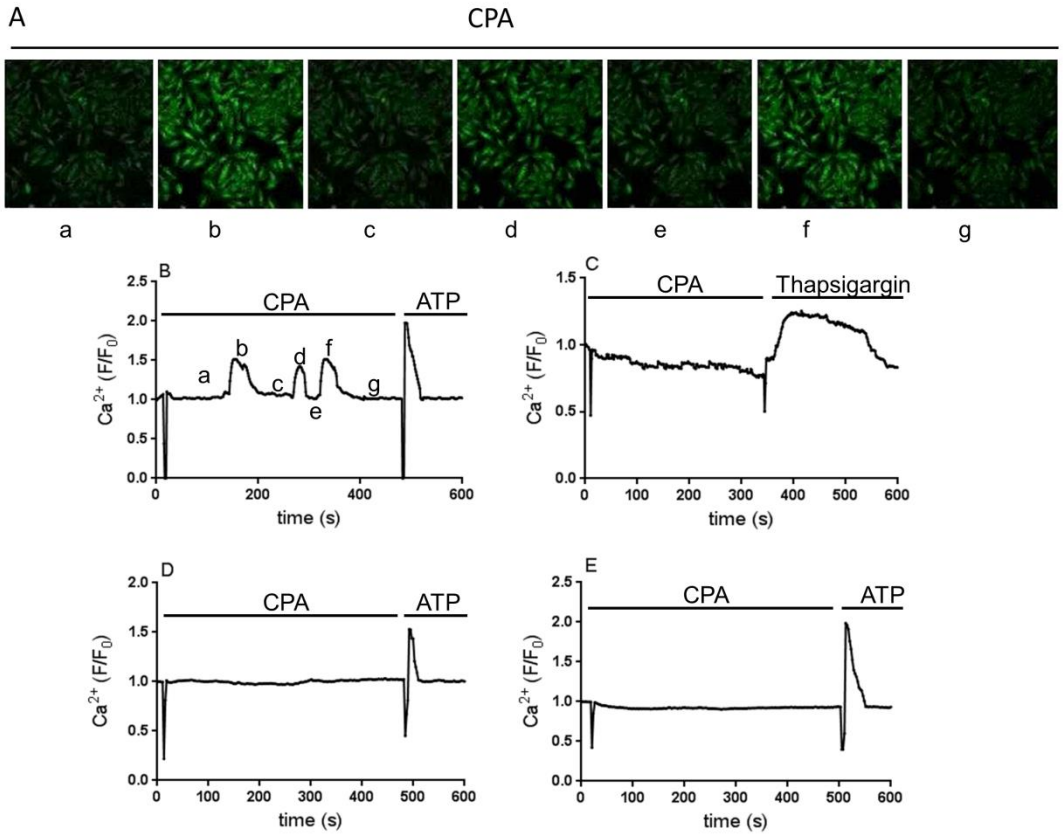
A
CPA
a
b
c
d
e
f
g
B
CPA
ATP
a
b
c
d
e
f
g
Ca^{2+} (F/F_0)
time (s)
C
CPA
Thapsigargin
Ca^{2+} (F/F_0)
time (s)
D
CPA
ATP
Ca^{2+} (F/F_0)
time (s)
E
CPA
ATP
Ca^{2+} (F/F_0)
time (s)

Figure 14

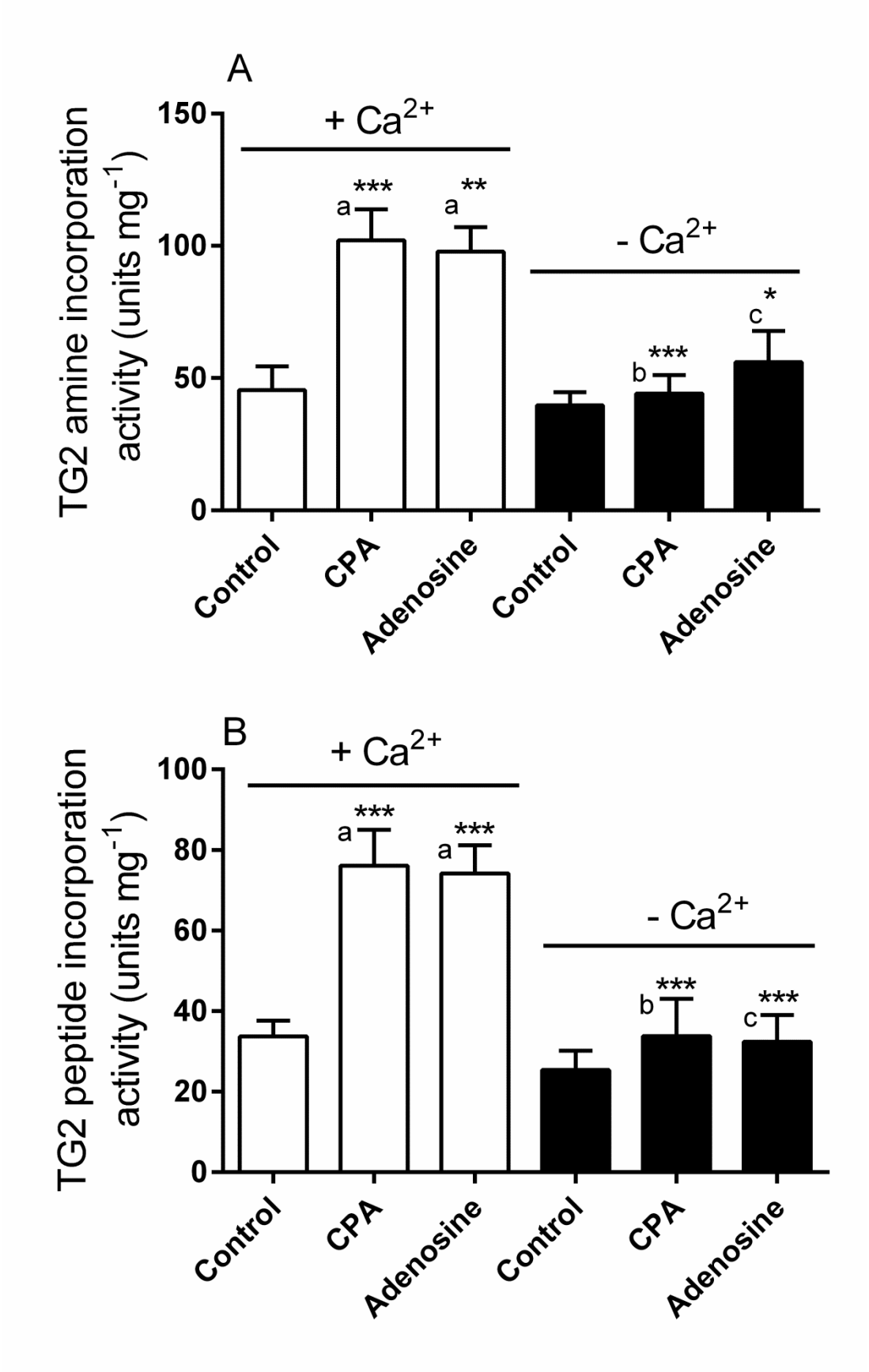
A
+ Ca2+
- Ca2+
TG2 amine incorporation activity (units mg-1)
150
100
50
0
***
**
a
a
b
c
*
***
Control
CPA
Adenosine
Control
CPA
Adenosine
B
+ Ca2+
- Ca2+
TG2 peptide incorporation activity (units mg-1)
100
80
60
40
20
0
***
***
***
***
a
a
b
c
Control
CPA
Adenosine
Control
CPA
Adenosine

Figure 15

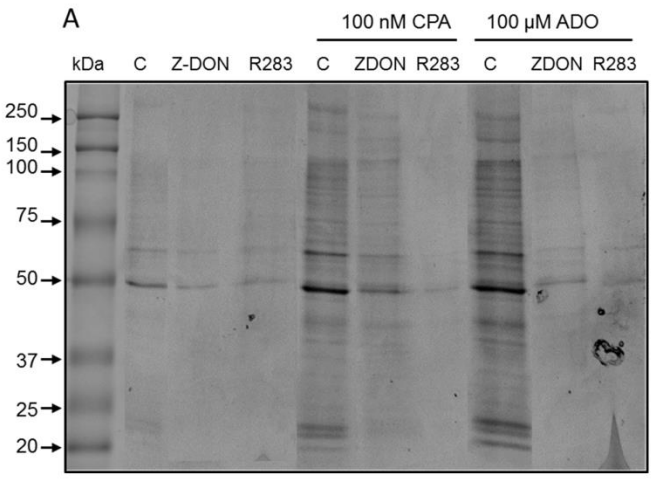
A
100 nM CPA
100 µM ADO
kDa
C
Z-DON
R283
C
ZDON
R283
C
ZDON
R283
250
150
100
75
50
37
25
20

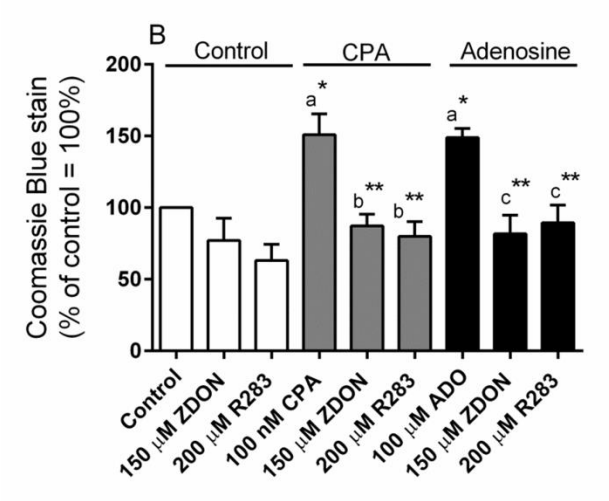
B
Control
CPA
Adenosine
Coomassie Blue stain
(% of control = 100%)
200
150
100
50
0
a *
b **
b **
a *
c **
c **
Control
150 µM ZDON
200 µM R283
100 nM CPA
150 µM ZDON
200 µM R283
100 µM ADO
150 µM ZDON
200 µM R283

Figure 16

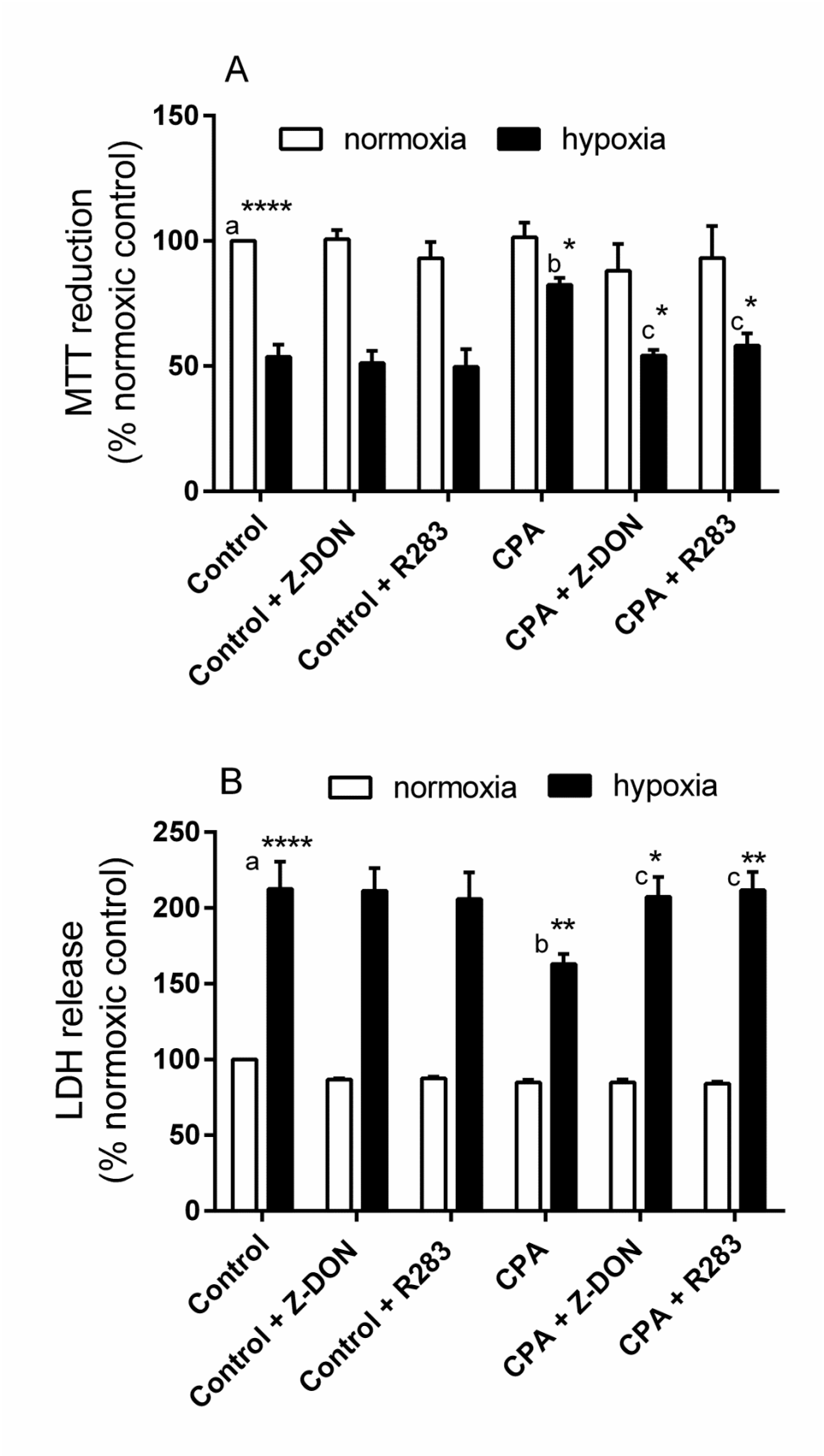
A
normoxia
hypoxia
MTT reduction
(% normoxic control)
150
100
50
0
a
****
b
*
c
*
c
*
Control
Control + Z-DON
Control + R283
CPA
CPA + Z-DON
CPA + R283
B
normoxia
hypoxia
LDH release
(% normoxic control)
250
200
150
100
50
0
a
****
b
**
c
*
c
**
Control
Control + Z-DON
Control + R283
CPA
CPA + Z-DON
CPA + R283